universe

MDPI

Review

High-Energy and Ultra-High-Energy Neutrino Astrophysics

Damiano F. G. Fiorillo

Niels Bohr International Academy, Niels Bohr Institute, University of Copenhagen, 2100 Copenhagen, Denmark; damiano.fiorillo@nbi.ku.dk

Abstract: The origin of high-energy cosmic rays, and their behavior in astrophysical sources, remains an open question. Recently, new ways to address this question have been made possible by the observation of a new astrophysical messenger, namely neutrinos. The IceCube telescope has detected a diffuse flux of astrophysical neutrinos in the TeV-PeV energy range, likely produced in astrophysical sources accelerating cosmic rays, and more recently it has reported on a few candidate individual neutrino sources. Future experiments will be able to improve on these measurements quantitatively, by the detection of more events, and qualitatively, by extending the measurement into the EeV energy range. In this paper, we review the main features of the neutrino emission and sources observed by IceCube, as well as the main candidate sources that could contribute to the diffuse neutrino flux. As a parallel question, we review the status of high-energy neutrinos as a probe of Beyond the Standard Model physics coupling to the neutrino sector.

Keywords: Neutrino astrophysics; high-energy neutrinos; cosmic accelerators; multi-messenger astronomy

1. Introduction

Neutrinos interact feebly with matter. This property, which makes them challenging to detect, also makes them a powerful probe of distant astrophysical environments, since they can reach Earth directly from the interior of the sources where they are produced. Neutrino astronomy can, therefore, provide an inside view of astrophysical sources. The most recent development in neutrino astronomy is high-energy (HE) neutrino astrophysics, mostly relating to neutrinos in the TeV-PeV range. They can be produced in the interactions of hadronic cosmic rays with dense targets of gas, dust, or low-energy photons. Therefore, cosmic neutrinos are a direct probe of the presence of hadronic cosmic rays in astrophysical sources.

The breakthrough in HE neutrino astronomy came in 2013 when the neutrino telescope IceCube reported the measurement of a diffuse neutrino flux between 100 TeV and 10 PeV of cosmic origin [1–5]. While the angular distribution of these neutrinos is consistent with isotropy, suggesting an extragalactic nature for their origin, the sources of this diffuse flux have not been conclusively elucidated. However, IceCube has reported on various significant advances, including a number of likely coincidences of neutrino detections with transient sources [6–8], and most recently the discovery of the first steady-state neutrino point source, the Seyfert galaxy NGC 1068 [9,10], and the discovery of a Galactic subdominant component of the diffuse flux. The interpretation of these results has stimulated a great deal of advances in the theoretical modeling of various source candidates. A parallel development has been the realization that HE neutrino observations can inform us about various Beyond the Standard Model (BSM) theories, especially connected with the neutrino sector. Since these neutrinos have much higher energies than the terrestrial ones, and they traverse long distances before reaching Earth, they are particularly sensitive to BSM physics at high-energy scales. However, extracting information on BSM physics, in light of the uncertainty on the astrophysical origin of HE neutrinos is challenging. In this paper, we

check for updates

Citation: Fiorillo, D.F.G. High-Energy and Ultra-High-Energy Neutrino Astrophysics. *Universe* **2024**, *10*, 149. https://doi.org/10.3390/universe10030149

Academic Editor: Salvatore Esposito

Received: 14 February 2024
Revised: 12 March 2024
Accepted: 15 March 2024
Published: 20 March 2024

will review the main theoretical results obtained on both the astrophysical and particle physics aspects of HE neutrinos.

Extending the IceCube measurements above the PeV, in the so-called ultra-high-energy (UHE) range, from 10 PeV to above the EeV, requires different experimental techniques, an effort undertaken by various collaborations. From the theoretical side, UHE neutrinos are expected to be produced by ultra-high-energy cosmic rays (UHECRs), either in the intergalactic space or inside the sources in which they are accelerated. Therefore, a future measurement opens exciting learning opportunities to pinpoint the origin of UHECRs. For this paper, we focus on the more theoretical aspects of UHE neutrino astrophysics. Other recent reviews on this subject include Refs. [11–13].

Our discussion will be structured as follows: in Section 2 we review the main microscopic processes by which neutrinos are expected to be produced in astrophysical environments. Section 3 is a brief discussion of the observed properties of the diffuse astrophysical neutrino spectrum, with a focus on how these properties should be interpreted in terms of astrophysical source properties. In Section 4 we discuss the main candidate sources for neutrino production. Finally, in Section 5 we discuss recent proposals to use high-energy astrophysical neutrinos as a probe of physics beyond the Standard Model.

2. Neutrino Production Processes

Hadronic cosmic rays interacting at high energies generally lead to the production of mesons, which in their decay lead to a neutrino emission. Since the lightest meson is the pion, neutrino production is most often associated with the decay of charged pions $\pi^+ \to \mu^+ \nu_\mu$ and the subsequent muon decay $\mu^+ \to e^+ \nu_e \overline{\nu}_\mu$. The precise mechanism by which pion production happens can either be purely hadronic, in pp collisions between cosmic rays and a dense target, or photohadronic, in $p\gamma$ collisions with a photon field. Heavier nuclei within CRs can also be subject to analogous collisions with matter or with radiation fields. As we will discuss later, astrophysical environments may exhibit both kinds of production mechanisms. The specific properties of the neutrino fluxes emitted depend on the process at hand; here we review what features are mainly expected in both cases.

Before delving into the peculiarities of each case, we briefly discuss what are the expectations for the parent cosmic-ray spectrum within neutrino sources. A detailed treatment should of course be conducted on the basis of each separate source class, but the general expectation is that cosmic rays are accelerated in their passage through moving magnetic inhomogeneities; various mechanisms involve shock wave acceleration, stochastic acceleration in magnetic turbulence, and acceleration in regions of magnetic reconnection. While no universal statement can be made, these acceleration mechanisms seem to generally lead to a CR spectrum behaving as a power law [14] $dN_p/dE_p \propto E_p^{-s_p}$ up to a maximum proton energy $E_{p,\mathrm{max}}$. The spectral index s_p depends on the acceleration mechanism; an often-used benchmark is $s_p = 2$, as expected from acceleration in non-relativistic shock waves [15], but different processes can actually lead to much harder spectra, with $s_p \sim 1$, or softer, with $s_p \sim 3$. The maximum energy $E_{p,\mathrm{max}}$ should be determined by the balance between the time it takes to be accelerated to $E_{p,\mathrm{max}}$ and the maximum time a particle can spend inside the acceleration region, or in the presence of strong cooling due to CR interactions with the cooling timescale. Thus, it is often assumed that within each source, CRs have a power-law spectrum with a cutoff.

Regarding the neutrino production processes, in pp collisions, pions are produced by deep inelastic scattering. The amount and spectrum of the produced pions require knowledge of hadronic physics and thus must be obtained from Monte Carlo codes based on phenomenological models of strong interactions, such as PYTHIA [16], QGSJETII-04 [17], and SIBYLL [18]. Analytical parameterizations are also available for the spectrum of π and η mesons in Ref. [19]. While the hadronic physics involved in these codes is certainly subject to uncertainties, since it is based on extrapolating the models tuned to reproduce measurements at the center-of-mass energies of LHC to higher energies, in astrophysical

environments the uncertainties on the source properties are usually the dominant source of uncertainty.

For simple estimates, it is usually enough to assume that pions carry an average fraction of the parent proton energy equal to $E_\pi \simeq E_p/5$, as seen from the Monte Carlo simulation of the scattering. Since in pion decay, four ultra-relativistic particles are produced, each neutrino on average carries an energy $E_\nu = E_\pi/4 \simeq E_p/20$. Since the total pp cross-section is itself not strongly dependent on energy above the threshold for pion production, the neutrino spectrum from pp collisions usually follows the parent proton spectrum. Given that many acceleration mechanisms are expected to produce power-law cosmic-ray spectra, with a typically soft spectral index $dN_p/dE_p \propto E_p^{-s_p}$ with $s_p \gtrsim 2$, this leads to a general expectation that pp sources should produce soft power-law neutrino spectra, although of course, this depends strongly on the assumption on the parent cosmic-ray spectrum.

From the point of view of the flavor composition of the produced neutrinos, from the pion decay chain, one then expects a so-called pion-beam flavor composition (f_e,f_μ, f_τ) = (1,2,0)/3, where f_α is the neutrino fraction in flavor α. Furthermore, since in pp collisions a roughly equal amount of π^+, π^-, and π^0 is produced, an equal fraction of neutrinos and antineutrinos is expected.

In $p\gamma$ collisions, pions can be produced if the center-of-mass energy exceeds roughly 0.2 GeV. If we denote by ε_γ and E_p the photon and proton energy, respectively, and we introduce the angle θ between the proton and photon momenta, the condition for the $p\gamma$ interaction can be written (Assuming $\varepsilon_\gamma \ll E_p$.) as $E_p\varepsilon_\gamma(1-\cos\theta) \gtrsim 0.04$ GeV^2, which depends on the angle between proton and photon. As shown in Ref. [20], after averaging the cross section over the angle, under the assumption of an isotropic photon target, the condition can be written as

$$E_p\varepsilon_\gamma \gtrsim \frac{m_p\epsilon_{\rm th}}{2}, \tag{1}$$

with m_p the proton mass and $\epsilon_{\rm th} \simeq 150$ MeV.

Just like pp processes, photohadronic processes too are generally described by means of numerical codes: the main tool for this task is the Monte Carlo code SOPHIA [21,22]. At low energies, the cross section is dominated by a number of resonances, the most prominent of which is the Δ-resonance (see, e.g., Ref. [23])

$$p+\gamma \to \Delta^+ \to \begin{cases} n+\pi^+ & 1/3 \text{ of cases} \\ p+\pi^0 & 2/3 \text{ of cases.} \end{cases} \tag{2}$$

A second contribution taken into account is the direct production of pions, which are mediated by the t-channel exchange of mesons. Finally, at higher energies, the dominant contribution is the so-called multi-pion production, due to the large number of pions in the final states.

The use of SOPHIA for the simulation of $p\gamma$ interactions can be time-consuming, just as in the pp case, so analytical approaches are often adopted. A commonly used approximation [24] is the use of the Δ-resonance contribution alone, assuming that each secondary carries a fixed fraction of the initial proton energy. For example, for pion production, it is assumed that an energy $E_\pi \simeq 0.22E_p$ is carried by the daughter pion [20]. Correspondingly, photons carry an energy $E_\gamma = E_\pi/2 \simeq 0.11E_p$ on average. Neglecting the multi-pion contribution in this approach, however, is not generally justified, as emphasized, e.g., in Refs. [20,25–28]. Analytical parameterizations for the final neutrino and gamma-ray spectra, including all contributions are given in Ref. [29].

For simple order-of-magnitude estimates, in $p\gamma$ production, it is still reasonable to assume that neutrinos carry an energy $E_\nu \simeq E_p/20$. On the other hand, the assumption that the neutrino spectrum follows the parent proton spectrum here breaks down because the interaction rate with photons is determined by the photon spectrum. For Δ-resonance interaction, the interaction rate at a proton energy E_p is determined essentially by the photon number density at the resonance energy $\varepsilon_\gamma \sim 0.2\ \text{GeV}^2/E_p$, while for multi-pion

interactions the interaction rate is determined by the integrated photon number above this energy [28]. If the photon spectrum is a soft power-law $dn_\gamma/d\varepsilon_\gamma \propto \varepsilon_\gamma^{-s_\gamma}$ with $s_\gamma > 1$, the resulting neutrino spectrum is typically hardened compared to the proton spectrum, behaving as $dN_\nu/dE_\nu \propto E_\nu^{-s_p+s_\gamma-1}$ [23]. This leads to a common expectation that if protons are accelerated with an E_p^{-2} spectrum up to a maximum energy $E_{p,\max}$, the resulting neutrino spectrum should be harder. Under this assumption, the neutrino energy density $E_\nu^2 dN_\nu/dE_\nu$ increases with energy, up to a maximum energy $E_{\nu,\max} \simeq E_{p,\max}/20$. The bulk of the energy injection is, therefore, emitted around a characteristic energy $E_{\nu,\max}$, producing spectral shapes similar to a bump [30].

Regarding the expected flavor composition of the produced neutrinos, in this case, the pion decay chain leads to a pion beam flavor composition; on the other hand, the neutrino-to-antineutrino ratio depends on the dominant production channel. While the multi-pion channel leads to a roughly equal amount of π^+ and π^-, and thus equipartition between neutrinos and antineutrinos; the Δ resonance channel breaks this symmetry and alters this simple prediction.

The discussion above refers to the simplest picture of neutrino production. This picture can be altered due to cooling in strong magnetic fields, and processes beyond pion production see, e.g., Refs. [20,22,23,26,28,31–35]. At sufficiently large magnetic fields, the intermediate muons and pions produced in the interaction may suffer large synchrotron losses before their decay, and therefore, become unable to produce high-energy neutrinos. Since muons are lighter and have a longer lifetime than pions, they are the first to suffer strong energy losses before decaying, at energies $E_\mu \gtrsim 4.8 \times 10^9$ GeV $(B/1\text{ G})^{-1}$, thus inversely depending on the magnetic field. Above these energies, only neutrinos from the primary pion decay can be produced at high energies, leading to a change both in the energy spectrum and in the flavor composition; the latter is now the so-called muon-damped composition $(0,1,0)$. The muons subject to strong losses are pushed to lower energies, just before the transition from a pion beam to muon-damped composition, and may produce in this energy region an excess of neutrinos from muon decay only, generating a so-called muon-beam flavor composition $(1,1,0)$. At large enough energies, pions may be subject to strong synchrotron losses, so a competing neutrino production channel is given by the decay of K mesons produced in the interactions. Finally, while pion decay is the main mechanism considered for neutrino production, an additional possibility is the decay of neutrons produced in pp and $p\gamma$ interactions. Since in neutron decay, neutrinos typically carry a very small fraction, of the order of 10^{-4} of the parent neutron energy, this production mechanism is most efficient at lower energies and is characterized by a neutron-beam flavor composition $(1,0,0)$.

3. The Diffuse High-Energy Neutrino Flux

In this section, we briefly review the main properties of the diffuse neutrino flux observed by IceCube. We separately discuss the energy spectrum, angular distribution, and flavor composition inferred from the observations. Finally, we review the connection between the diffuse neutrino and gamma-ray flux observations.

3.1. Energy Spectrum

Since the first observation of a diffuse (namely distributed all over the sky) high-energy neutrino flux from IceCube in 2013, the IceCube Collaboration has provided various updated measurements [1–4,36–38] of the properties of the flux. A key strategy is the use of different data selections which have complementary advantages and disadvantages in the energy resolution, background rejection, and overall number of events. The identification of the astrophysical component was originally performed with the High-Energy Starting Events (HESE) [38], namely events with an interaction vertex completely contained within the instrumented volume. This strategy allows a considerable rejection of atmospheric

muon and neutrino backgrounds and is particularly sensitive to cascade events produced mostly by ν_e and ν_τ. Another strategy consists of considering track events originating also outside of the detector from the northern sky (throughgoing muons) [39], which allows the rejection of atmospheric muons. Track events have a significantly better angular resolution, so they provide an improved sensitivity to point sources. A final analysis reported by the collaboration used contained cascade events only [5], which entirely eliminates the background of atmospheric muons and provides a measurement down to the tens of TeV range.

Most analyses of these measurements rely on a power-law fit to the neutrino spectrum of the form

$$\frac{d\Phi_\nu}{dE_\nu d\Omega} = \Phi_\nu \left(\frac{E_\nu}{100\ \text{TeV}} \right)^{-s_\nu} \tag{3}$$

While a power law is a natural expectation for certain classes of sources, as we have discussed in Section 2, it is not necessarily a good theoretical assumption for the entirety of the diffuse flux. Nevertheless, a power-law fit remains a reasonable characterization of the properties of the data, especially in view of the current experimental uncertainties. The values inferred for the parameters Φ_ν and s_ν from different data samples are summarized in Figure 1. The values inferred, especially for the spectral index are not in complete agreement, which may be attributed to systematic differences in the coverage of each data sample, e.g., sensitivity to different flavors or different regions of the sky. Nonetheless, they provide a roughly consistent picture of the high-energy neutrino flux.

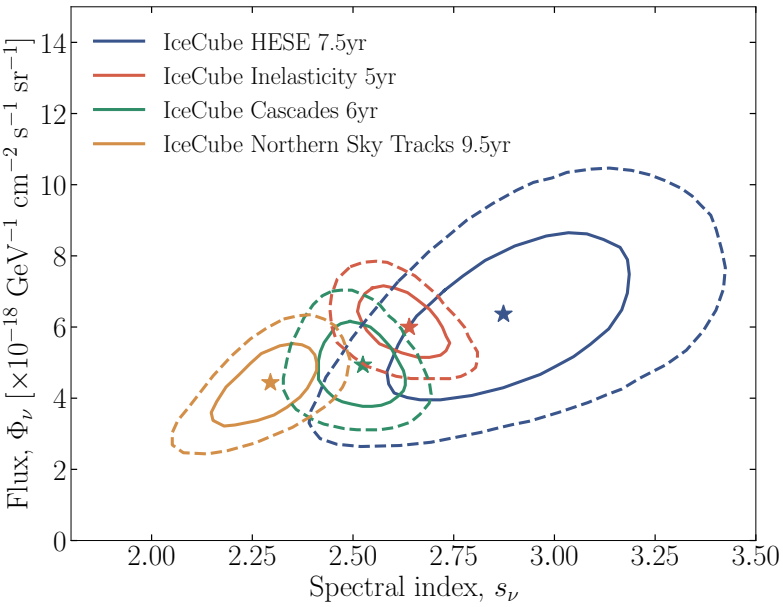

Figure 1. Inferred power-law parameters for the diffuse astrophysical neutrino flux; we show the flux normalization Φ_ν at 100 TeV and the spectral index s_ν. Different colors refer to different IceCube analyses, including the most recent HESE study [38], IceCube's 5 yr inelasticity measurement [40], the 6yr cascade sample [5], and the 9.5 yr track sample preliminary result [39]. Solid (dashed) lines are the 68% (95%) confidence level regions.

So far, the different data samples all seem to provide a general agreement with the power-law fit. Only very recently, did preliminary IceCube analyses report on the first hints of non-power-law behavior from a combined analysis of the cascades and tracks data sample, showing a hardening of the spectrum in the tens of TeV range [41]. Above hundreds of TeV, the relatively limited statistics make it challenging to identify deviations from

a power law. Such deviations could be expected if the diffuse flux comes from the superposition of multiple source classes, each with their own spectrum, e.g., in scenarios where photohadronic "bumps" dominate at PeV energies with a power-law flux below PeV (see, e.g., Refs. [42,43]), but larger statistics will be crucial to test these multicomponent pictures.

3.2. Angular Distribution and Point Sources

The angular distribution of astrophysical neutrinos may help identify their origin. If neutrinos are produced in extragalactic sources, they should show an angular distribution, on average isotropic, with clustering around the positions of their sources. On the other hand, a Galactic component, produced in pp interactions of Galactic cosmic rays with interstellar material, should show a clear correlation with the Galactic Center.

So far, the angular distribution of the astrophysical neutrinos detected by IceCube seems to be mostly isotropic. Only very recently, a subdominant component has been identified as Galactic, since its spatial distribution matches the expected one. The remaining part of the flux is, therefore, most likely extragalactic, with recent studies confirming that even the flavor composition is consistent with isotropy [44]. In order to identify its sources, the IceCube Collaboration adopts different strategies, including searches for multiplets of events from similar directions in the sky [9,45–48], cross-correlation of neutrino angular distribution with catalogs of known sources [49–62] and with ultra-high-energy cosmic rays [63–65], the analysis of the neutrino angular power spectrum [66–69], and searches for temporal and spatial correlations with transient sources [70,71]. Up to now, the IceCube Collaboration has reported on the detection of two sources, the Seyfert galaxy NGC 1068 [10], and the blazar TXS 0506 + 056 [6,7]. In addition, a number of spatial and temporal coincidences of individual high-energy neutrinos with tidal disruption events have been reported [8,72,73] which, however, are less conclusive.

The presence, or absence, of clustering in the neutrino angular distribution can provide important information on the nature of the neutrino sources [74–77]. A large degree of clustering, with neutrinos appearing in multiplets from similar directions, would suggest that the sources of the diffuse neutrino flux are rare and individually powerful. On the other hand, so far the high-energy neutrino sky above 100 TeV seems to show the opposite regime, with no multiplets detected. This allows us to set upper bounds on the neutrino luminosity of individual sources L_ν, depending on the effective source density $\rho_{\rm eff}$; these are shown in Figure 2. Since the product $L_\nu \rho_{\rm eff}$ directly determines the magnitude of the diffuse neutrino flux, these bounds allow us to infer a maximum luminosity for the sources dominating the neutrino sky, and even to exclude some candidate source populations already with the present-day IceCube data. A similar approach might also be helpful in the UHE range above tens of PeV, where there are at present no observations but where a sufficient sensitivity for detection may be reached in the next decade by radio telescopes; using the predicted angular resolution of these experiments, their potential sensitivity to point source detection has been analyzed in Refs. [78,79]. On the other hand, one should emphasize that all these conclusions rely on the assumption of a single population of identical sources, although there are attempts to use the angular information in multi-component studies [80].

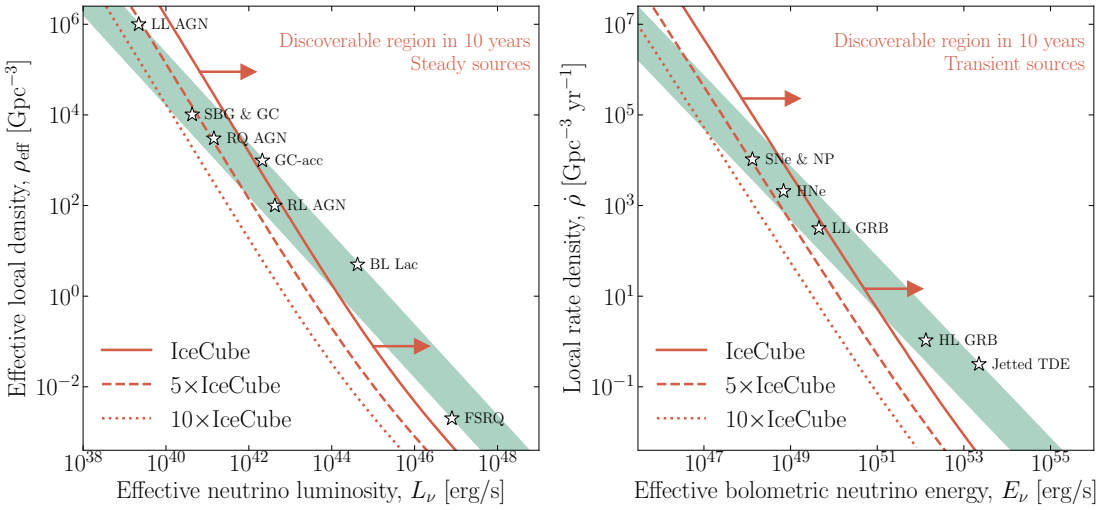

Figure 2. Multiplet constraints on astrophysical source populations, both steady (**left**) and transient (**right**). The green band identifies the region needed to explain the bulk of the IceCube flux, depending on the assumed redshift evolution. The red lines show regions that should be discoverable with IceCube in 10 years (solid), with an exposure 5 times (dashed) and 10 times (dotted) larger. We highlight several candidate populations by the neutrino luminosity needed to saturate the diffuse neutrino flux; they include low-luminosity AGN (LL AGN), starburst galaxies (SBG), galaxy clusters (GC), galaxy clusters with acceleration in accretion shocks (GC-acc), radio loud AGN (RL AGN), BL Lacs, flat-spectrum radio quasars (FSRQ), supernovae (SNe), newborn pulsars (NP), hypernovae (HNe), low-luminosity GRBs (LL GRB), high-luminosity GRBs (HL GRB), jetted tidal disruption events (TDE). Figure reproduced from Ref. [81].

3.3. Flavor Composition

Neutrino detection in IceCube does not allow the identification of the flavor of each individual event. Nevertheless, sensitivity to the flavor composition of the astrophysical flux can still be achieved using the different topologies of the observed events [40,82–87]. Electron and tau neutrinos typically give rise to cascade events contained in the detector. Muon neutrinos can either produce a cascade, in the case of neutral-current scattering with nuclei, or a track originating from the muon produced in charged-current scatterings. Contamination of tracks from the charged-current scattering of tau neutrinos can also appear due to the tau rapidly decaying into a muon with a branching ratio of 17%. Thus, simultaneous analysis of tracks and cascades allows for a partial discrimination of the flavor composition.

At higher energies, charged-current scattering of tau neutrinos can also induce a characteristic topology, typically called a double bang, with two cascades separated by a track corresponding to the propagation of the unstable tau lepton. The IceCube Collaboration reported the first observation of two candidates for double bang events in 2020 [88], allowing to obtain updated constraints on the flavor composition and to determine the existence of a tau component in the astrophysical neutrino flux.

A separate flavor-dependent detection process is the neutrino-electron resonant scattering $\overline{\nu}_e e^- \to W \to X$, where X is a generic final state. The cross-section for this process has a resonance peak, known as Glashow resonance, for an antineutrino energy (in the rest frame of the electron) of 6.3 PeV, leading to an expected excess of events around that energy. In 2020, IceCube reported the detection of a cascade event consistent with the properties expected for a Glashow resonance [89]. The detection of a Glashow resonance event not only provides information on the flavor of the neutrino but also gives a unique way to discriminate between neutrinos and antineutrinos and learn about their production processes [90,91].

Interpreting these results on the flavor composition in terms of astrophysical mechanisms of production, one should be careful in considering the impact of neutrino mixing. As we have discussed in Section 2, at the source neutrinos can be produced in a variety of conditions, resulting in flavor regimes that include the pion beam, the muon-damped regime, the muon beam, and the neutron beam. All these regimes have in common the absence of tau neutrinos since the associated tau lepton would require very large center-of-mass energies as a threshold for production; nevertheless, in special cases associated with charm production, this could possibly happen. Once neutrinos are produced with a given flavor composition f_α at the source, they propagate in a vacuum from the source to Earth. Since the oscillation lengths are much smaller than the propagation distance, they quickly decohere, evolving into a new flavor composition

$$f_\alpha^\oplus = \sum_{i,\beta} |U_{\alpha i}|^2 |U_{\beta i}|^2 f_\beta, \tag{4}$$

where U is the Pontecorvo–Maki–Nakagawa–Sakata (PMNS) mixing matrix [92,93]. Thus, for example, for most production scenarios, tau neutrinos at Earth can only be observed in the presence of mixing. Accounting for neutrino mixing, the difference among different flavor compositions at the source is largely reduced, challenging a clear discrimination among different mechanisms. Nevertheless, flavor can certainly inform us about the neutrino production mechanisms [26,31,32,94–105]; the increase in statistics connected with future neutrino telescopes will provide a significant improvement to this picture [106]. Even more importantly, future observations should be able to test scenarios with energy-dependent transitions among different flavor regimes [91], which, as discussed in Section 2 are the most natural expectation for models with non-trivial flavor compositions.

3.4. Multimessenger Connections

The diffuse high-energy neutrino flux is produced from cosmic-ray interactions, and in all such interactions, gamma-rays should be produced as well. Therefore, a connection between these three messengers can intuitively be expected. This expectation is strengthened by the observation that the energy flux observed on Earth in all three messengers seems to be comparable, as shown in Figure 3. So, from the observational side, a scenario that can simultaneously explain the signal of all three messengers would be appealing [107]. Nevertheless, from the theoretical side, the precise connection between the different messengers is rather model-dependent.

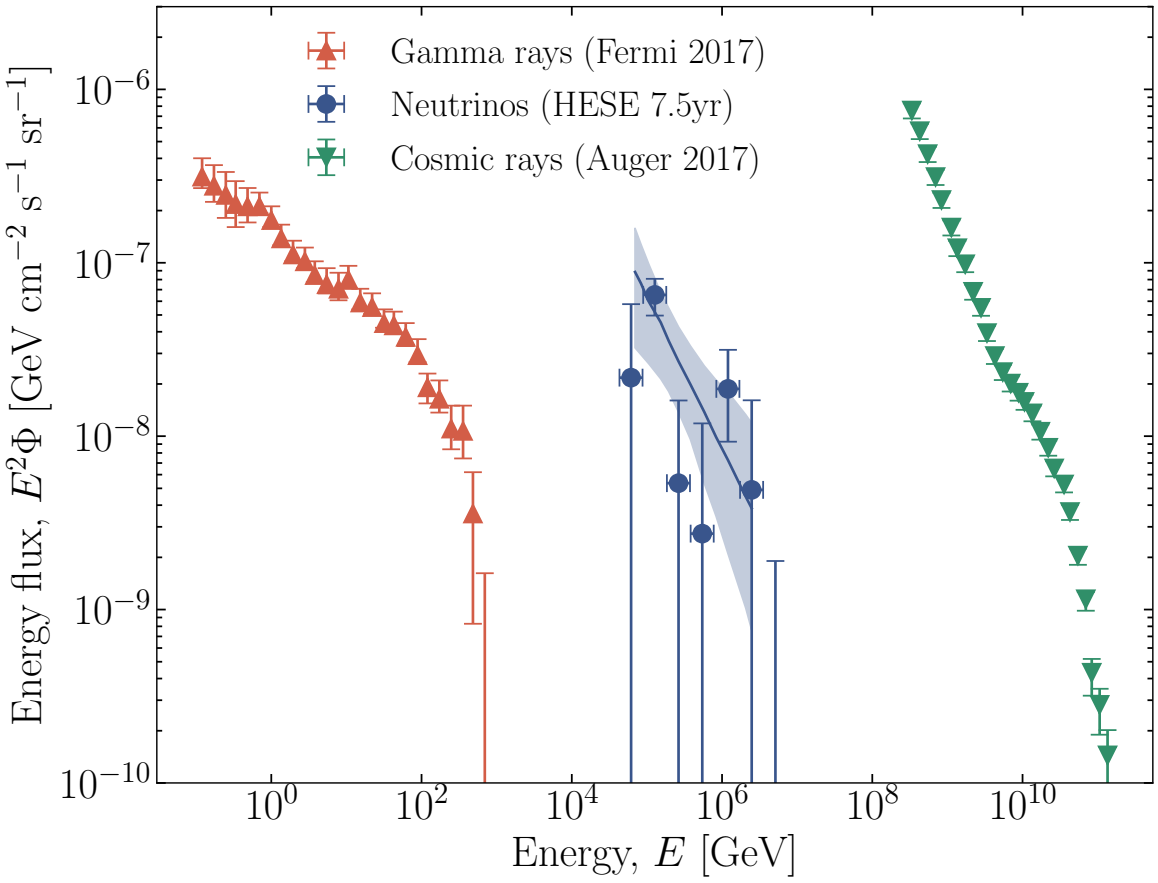

Figure 3. High-energy fluxes of gamma rays, neutrinos, and cosmic rays. Figure reproduced from Ref. [38]; gamma-ray measurements are from Fermi [108] while UHECR measurements are from the Pierre Auger Observatory [109].

A direct connection between the observed neutrino flux and the UHECR flux should exist if the sources of IceCube neutrinos simultaneously produce the observed UHECRs. A necessary requirement for this self-consistent picture is that the sources should allow a sizable fraction of UHECRs to escape so that they can reach Earth. Following this picture, Waxman and Bahcall [110,111] derived an upper bound on the neutrino flux $E_\nu^2\Phi_\nu \lesssim 2\times10^{-8}$ GeV cm^{-2} s^{-1} sr^{-1}, assuming an E^{-2} UHECR flux normalized to the observed flux at Earth, and maximum efficiency for neutrino production from UHECRs. Such a bound cannot be evaded if the neutrino sources are simultaneously the sources of UHECRs. On the other hand, the neutrino flux observed by IceCube seems to be comparable with the Waxman–Bahcall bound, perhaps suggesting that they are not produced in environments transparent to UHECRs, but rather in reservoirs that can confine CRs, such as starburst galaxies (see Section 4.4). An intriguing possibility is that the fraction of escaping CRs is energy-dependent, which can be realized in models of galaxy clusters (see Section 4.5) where CRs below about 100 PeV are confined and can produce a large neutrino flux, while those above 100 PeV escape and contribute to the UHECR flux.

The connection between neutrinos and gamma rays is similarly dependent on the properties of the producing environment. All the hadronic processes proposed to explain neutrinos rely on pion production. The decay of charged pions produces neutrinos, while the decay of neutral pions produces gamma-rays, so one could expect a direct proportionality $E_\nu^2\Phi_\nu \propto E_\gamma^2\Phi_\gamma$, where the proportionality factor depends on the relative proportion of charged and neutral pions and can be slightly different for pp and $p\gamma$ scenarios. However, this simple conclusion is affected by two factors.

First, even if gamma-rays are produced and are able to escape the source, above about 1 TeV they are strongly attenuated in the extragalactic space due to their $\gamma\gamma$ interaction with the Cosmic Microwave Background (CMB) and Extragalactic Background Light (EBL). Their energy is then cascaded below the TeV region and contributes to the high-energy gamma-ray flux observed by Fermi-LAT. This is the expected scenario in models of pp sources, e.g., starburst galaxies and galaxy clusters, which are generally expected to be gamma-ray transparent. In this case, the amount of energy that is cascaded in sub-TeV gamma-rays is particularly sensitive to the neutrino spectral index s_ν, where $\Phi_\nu \propto E_\nu^{-s_\nu}$. Normalizing the neutrino spectrum to the observed IceCube flux in the 100 TeV–10 PeV range, a soft spectrum implies a larger amount of energy below 100 TeV; the corresponding gamma-ray flux, after being reprocessed by the cascade, could easily exceed the Fermi-LAT observations. As shown in Ref. [112], this imposes an upper bound on the spectral index $s_\nu \lesssim 2.1 - 2.2$ for pp sources to explain the neutrino flux above 100 TeV and be consistent with the gamma-ray data. It also implies that gamma-ray transparent sources are difficult to reconcile with the neutrino flux between 10 TeV and 100 TeV [113–115].

Second, the sources themselves may not be gamma-ray transparent. This is a natural expectation for efficient $p\gamma$ sources since the dense target of photons needed for $p\gamma$ interactions is also a target for $\gamma\gamma$ absorption and subsequent cascading [113,116–118]. A population of gamma-ray opaque sources may easily explain the neutrino flux below 100 TeV without exceeding the GeV–TeV Fermi-LAT observations [113–115]. Candidate sources with these properties are choked gamma-ray bursts [119,120] and active galactic nuclei (AGN) cores [121,122]. In this sense, the detection of a neutrino signal from the AGN NGC 1068 may provide a first hint that AGN cores are responsible for the bulk of the neutrino production in the 10 TeV–100 TeV range, a scenario that can be accommodated with the current neutrino production models in AGN coronae [123,124].

4. Astrophysical Sources of Neutrinos

Historically, the first candidate sources for neutrino production were looked for among those sources expected to produce UHECRs, e.g., gamma-ray bursts and blazars. However, in more recent years novel source classes have been explored. Here, we provide a brief review of the main source classes considered in the literature, focusing especially on the most recent developments motivated by experimental observations.

4.1. Active Galactic Nuclei

AGN are bright compact regions at the center of host galaxies. Their electromagnetic (EM) emission spans all frequency bands of the spectrum and can reach luminosities as large as 10^{47} erg/s. This emission is believed to be powered by the accretion of matter onto a central supermassive black hole (SMBH) [125], but the mechanism by which the gravitational energy of the infalling matter can be converted into the wide variety of observed energy emission processes is not conclusively understood. Indeed, while AGN are all likely characterized by a central SMBH, they exhibit a wide variety of behaviors and are characterized in multiple subclasses. From the point of view of neutrino emission, a primary distinction can be made between jetted and non-jetted AGN. The former (typically ∼1–10% of the population) may exhibit powerful jets with large radio luminosities, while the latter are radio-quiet, and may have weak jets inferred from radio observations. Among jetted AGN, a special class is constituted by blazars, for which the jet points directly to Earth. In the following, we separately discuss the two classes; for a more detailed review of neutrino emission in AGN, see, e.g., Ref. [126].

4.1.1. Non-Jetted AGN

Non-jetted AGN are typically characterized by a bright optical-ultraviolet (OUV) emission likely produced from an optically thick, geometrically thin accretion disk around the SMBH. They may also exhibit bright X-ray emission, which is usually explained by a coronal region closer to the SMBH where a population of energetic electrons is able to

Comptonize the disk radiation. In order to maintain a stationary population of energetic electrons, some energization mechanism, most likely of magnetic origin is needed, which suggests that the corona may be strongly magnetized.

While neutrino production in the AGN inner regions has long been suggested [127–129], this topic has received considerable momentum from the IceCube discovery of an excess of the neutrinos from the direction of the Seyfert galaxy NGC 1068. The observed neutrino signal is consistent with a power-law flux $d\Phi_\nu/dE_\nu \propto E_\nu^{-3.2}$, and a neutrino luminosity of the order of 10^{42} erg/s [10]. This is more than an order of magnitude larger than the upper bounds set by MAGIC on the gamma-ray luminosity at the same energy [130], indicating that neutrinos are produced in an optically thick region that absorbs gamma rays [131]. The coronal region would be an ideal candidate, due to the dense X-ray photon field which renders it gamma-ray opaque via $\gamma\gamma$ processes. Various acceleration mechanisms have been proposed to explain the formation of a non-thermal proton population, including diffusive shock acceleration [132], stochastic acceleration in magnetic turbulence [122,133], and magnetic reconnection [124,134]. Independently of the acceleration model at work, the coronal region would efficiently lead to neutrino production either via pp collisions with the material in the coronal region or via $p\gamma$ collisions with the coronal X-rays and possibly the OUV photons from the accretion disk. Alternative sites for neutrino production have also been considered, such as failed line-driven winds, where protons may be accelerated by diffusive shock acceleration [135], the inner torus, and the interaction region between the weak jet and the interstellar material [136]. All the proposed scenarios share the common features of gamma-ray opaqueness, needed to explain the stringent upper bounds on the GeV gamma-ray luminosities. However, the energy injected in high-energy gamma rays is not lost but is rather reprocessed into MeV photons via the electromagnetic cascade initiated by $\gamma\gamma$ processes. Therefore, future measurements of the MeV emission from NGC 1068 will provide a critical test for many of these scenarios. Finally, while regions close to the SMBH are likely needed to explain the gamma-ray opaqueness associated with the signal of NGC 1068 [137], sub-dominant neutrino production could also be associated with outer regions, e.g., the ultra-fast-outflows driven by the AGN activity [138,139].

4.1.2. Blazars

Jetted AGN host powerful non-thermal emission, with most of the power strongly beamed along the direction of the jet. For blazars, with the jet pointing to Earth, the spectral energy distribution spans across the entire frequency spectrum, and is typically organized in two humps; a low-energy hump, typically attributed to synchrotron radiation from electrons accelerated in the jet, and a high-energy hump, whose origin is more debated. In a purely leptonic scenario, the second hump is explained by inverse Compton scattering off the synchrotron photons, while in hadronic scenarios it can be explained by the cascade resulting from photons and leptons injected by $p\gamma$ interactions [140] or by synchrotron emission from cosmic rays [141,142].

In most blazar models, neutrino production is typically predicted via $p\gamma$ interactions. If hadronic cosmic rays are accelerated in blazar jets, then synchrotron photons from coaccelerated electrons, forming the first hump are a natural target for photohadronic neutrino production [143,144]. They are the dominant target in models for BL Lacertae (BL Lac) objects, which are typically blazars with low luminosity. For the class of Flat Spectrum Radio Quasars (FSRQs), external photon fields, whose nature is model-dependent, may provide a dominant target for $p\gamma$ [145]. Since the interaction is likely photohadronic, a standard E_p^{-2} expectation for the CR spectrum translates into a hard neutrino spectrum $E_\nu^{-s_\nu}$, with $s_\nu < 2$, which is a common feature of most blazar emission models. The cutoff of the neutrino spectrum is then directly determined by the maximum acceleration of the accelerated CRs. The neutrino luminosity is expected to be higher for sources bright in the gamma rays, but the precise scaling is model-dependent; for leptonic models, assuming that the CR luminosity $L_{\rm CR}$ is proportional to the bolometric non-thermal luminosity of the jet $L_{\rm rad}$, the neutrino luminosity is expected to scale as $L_\nu \propto L_{\rm CR} L_{\rm rad} \propto L_{\rm rad}^2$ if the $p\gamma$ target is the synchrotron field, as expected for BL Lacs and lower-luminosity objects, while $L_\nu \propto L_{\rm rad}^{3/2}$

if the $p\gamma$ target is an external photon field, as expected for FSRQs [146]. If the observed gamma-rays are instead of hadronic origin, we should rather expect $L_\nu \propto L_\gamma$ [147,148].

Blazars have been considered as candidates for the acceleration of UHECRs and neutrino production [144,145,149–151]. In such models, they must be able to accelerate CRs up to hundreds of EeV, so neutrino production would be expected mainly in the EeV region. In this scenario, the fraction of CR energy that results in EeV neutrino production likely depends on the source luminosity, with BL Lacs leading to a larger fraction of CRs leaving the source and contributing to the observed UHECR flux, and the brighter FSRQs more efficiently producing UHE neutrinos [146,152,153]. At present, IceCube is less sensitive in the EeV region than in the PeV one, so for now only the upper bounds on the neutrino flux have been set [154], which allows to constrain the source models. However, a significant improvement in sensitivity in this energy region will come from the future radio telescopes for UHE neutrinos, which will allow us to critically test the assumption of UHECR acceleration in blazar jets. In any case, in these scenarios where blazars can accelerate UHECRs, they quite likely are not the dominant source of IceCube neutrinos, since their predicted hard spectrum, if normalized to the IceCube observations, would exceed even the present-day upper limits on the UHE neutrino flux. One could, of course, relieve the assumption that blazars should simultaneously produce UHECRs and neutrinos, and consider scenarios in which they only accelerate CRs up to hundreds of PeV and produce neutrinos in the 100 TeV–1 PeV range. Even this picture is strongly constrained, both by the predicted hard neutrino spectrum in blazars and by stacking [53,155–157] and multiplet constraints (see Section 3.2), although unresolved blazars could still dominate the PeV neutrino flux [158].

The connection between blazars and neutrino production has received a significant boost from the detection [7] in September 2017, of a high-energy neutrino in spatial and temporal coincidence with the blazar TXS 0506 + 056 during a gamma-ray and X-ray flare. The coincidence was estimated at the 3σ level of significance. Furthermore, an analysis of archival data showed evidence [6] of a neutrino flare in the period from September 2014 to March 2015, without a corresponding electromagnetic flare, with an estimated significance of 3.5 σ, although when such an excess is searched for over the entire sky, it becomes insignificant [71]. The interpretation of these results in terms of astrophysical models seems to be challenging. For the 2017 flare, the necessary neutrino production would induce an electromagnetic cascade that is strongly constrained by the X-ray measurements [159–163]. For the 2014–2015 flare the situation is even more challenging due to the absence of a corresponding flare either in gamma-rays or X-rays and is difficult to reconcile with the expected electromagnetic cascade flux, at least in the context of one-zone models [161,164,165]. The detection of future neutrino-blazar coincidences will, therefore, be crucial to clarify the situation [166].

4.2. Gamma-Ray Bursts

Gamma-ray bursts (GRBs) are among the most energetic explosions in the Universe. A general discussion of their observational properties and theoretical mechanisms can be found, e.g., in Ref. [167]. First detected via their bright gamma-ray emission, they are characterized by a prompt emission with a duration ranging from below a few seconds, for short GRBs, and up to 10–1000 s for long GRBs. The energy ejected in the explosion is typically of the order of 10^{51} erg, and is believed to be emitted in highly collimated jets, whose origin may be associated either with a central black hole or with a strongly magnetized neutron star. The prompt emission is followed by an afterglow, with emission spanning all bands from radio waves up to gamma rays, lasting hours or days.

The presence of a jet is immediately suggestive of particle acceleration, an idea that is immediately confirmed by the observed power-law spectra, suggesting non-thermal emission. The traditional picture of GRBs is thus the following [168,169]: an initial event, which can be the collapse of a massive star for long GRBs or the mergers of two neutron stars for short GRBs, forms a central compact object and launches a jet. The jet has highly

relativistic velocities and can accelerate particles through various mechanisms, with the most widely proposed acceleration by the Fermi mechanism at shocks in hydrodynamical jets and acceleration via magnetic reconnection in strongly magnetized jets. If the acceleration occurs in optically thin regions, the accelerated non-thermal electrons can produce high-energy gamma rays via synchrotron radiation and/or inverse Compton radiation. Alternatively, if most of the energy dissipation takes place in an optically thick part of the jet, the saturated Compton cooling model appears to accurately match the observed spectra of at least some GRBs. At present, the energy dissipation and radiation mechanisms operating in GRB jets are still the subject of an open debate, and there is no single model that can account for all the prompt emission observations. At large distances, after the jet sweeps up an amount of mass comparable to its own energy, it starts a deceleration phase in which the shock waves propagates through the ambient medium. This is the traditional interpretation of the afterglow.

Regardless of the precise mechanism by which electrons are accelerated, if ions are accelerated as well, then one is led to investigate the possibility that GRBs could accelerate UHECRs [170–176] and produce high-energy neutrinos [24,172,175–185]; we refer also to Ref. [186] for a recent review of the connection between GRBs and high-energy neutrinos. Neutrino production in the prompt phase could happen via $p\gamma$ scattering on the observed gamma-ray flux, although the corresponding neutrino fluxes are subject to large uncertainties. In photospheric models, if CRs are accelerated they may still give rise to an observable neutrino signal [119,187,188], although sub-photospheric shock acceleration to high energies may be inefficient due to the radiation-mediated nature of the shocks. Even in this case, if CRs are not accelerated, neutrino production may still happen due to neutron–proton collisions, although in this scenario the neutrino emission would be most easily observed in the GeV-TeV region [189–191]. Finally, during the afterglow, due to the larger distances involved, ions can be accelerated to UHE, leading to the production of EeV neutrinos [185,192–195]. From the observational viewpoint, IceCube and other neutrino telescopes have not detected any temporal or spatial coincidence among the observed neutrinos and the known GRBs, allowing to establish limits on GRB neutrino emission [49,196–200], so the contribution of GRBs to the IceCube flux is limited to less than $\sim$1%. Comparable constraints have been derived from the non-observation of neutrinos [201] from the brightest GRB observed in October 2022, GRB 221009A [202–204]. These bounds strongly constrain the amount of baryons accelerated in GRBs, and therefore, their contribution to UHECRs, although they can be alleviated in multi-zone models. Furthermore, they do not apply to low-luminosity GRBs, which may not appear in the samples and could still contribute sizably to the UHE neutrino and UHECR flux [182,205–207]. Finally, choked GRBs, where the jet is not able to make it out of the stellar material, have been suggested as a candidate gamma-ray opaque source explaining the 10–100 TeV observed neutrino emission [119,120].

4.3. Tidal Disruption Events

A tidal disruption event (TDE) results from the accretion of material from a star torn apart by a supermassive black hole. The accretion can power electromagnetic emissions lasting for typical timescales of months to years. For some TDEs, the emission is accompanied by a powerful jet, as in the case of Sw 1644 + 57 [208]. One may, therefore, expect that in such jets, CR acceleration can power neutrino emission [209–212], although non-jetted TDEs have also been suggested as neutrino emitters [213,214]. The seminal proposal for UHECR acceleration and neutrino emission in TDEs was given in Refs. [215,216].

Neutrino production in TDEs gained interest with the association of three IceCube alerts with the candidate TDEs AT2019dsg [8], AT2019fdr [72], and AT2019aalc [73], although for some of them the identification as TDE is controversial [217]. If these associations are confirmed, they share some similarities; in all cases, the neutrino events were detected about 150–300 days after the peak in the optical-ultraviolet (OUV) emission of the events, and all events exhibited high OUV luminosities and a delayed infrared (IR) emission,

explained as OUV and X-ray radiation reprocessed by dust (dust echo). The neutrino signal could then be explained from $p\gamma$ interactions of accelerated CRs with either X-ray, OUV, or IR target [72,73,213,214,218–221], with the latter scenario potentially providing an explanation for the time delay and the presence of a strong dust echo in all cases.

4.4. Starburst Galaxies

Starburst galaxies (SBGs) are galaxies with an unusually high rate of star formation, which can reach values of 100 $M_\odot$ yr^{-1} (for comparison the average value in the Milky Way is around 3 $M_\odot$ yr^{-1}) [222]. Star-forming processes happen mostly in the nuclei of the galaxies, with typical dimensions of hundreds of parsecs. The presence of enhanced star-forming processes is generally connected with a large amount of interstellar material, with average number densities of 100 cm^{-3}. Due to these properties, SBGs exhibit enhanced far-infrared luminosities, with energy densities $U \sim 10^3$ eV cm^{-3}, and higher supernova rates, of the order of 0.1–1 yr^{-1}, compared to normal galaxies. Simulations have also shown that SBGs can have very large interstellar wind velocities of hundreds to thousands of kilometers per second [223,224].

The properties just discussed make SBGs very promising sources of hadronic neutrino and gamma-ray production. The large amount of ISM is an ideal target for pp collision, and the enhanced supernova rate suggests the presence of acceleration sites within the galaxy. For this reason, neutrino production in SBGs has been studied in the literature by various authors [43,112,225–235]. The scenario is typical of cosmic reservoirs, where supernovae embedded in the SBG accelerate CRs via DSA, and the CRs undergo pp collisions with the ISM. Since the typical timescale for pp collisions is much smaller than the escape time of CRs at large enough energies, the SBG acts as a calorimeter, where the CRs dump all of their energy in neutrino and gamma-ray emission [225,236]. Since this is a very efficient way of producing neutrinos, this mechanism can contribute significantly to the IceCube neutrino emission above 100 TeV, although in order to explain also the 1–10 PeV neutrinos, CRs should be accelerated to more than 100 PeV, which could be achieved by hypernovae [112,227,229], enhanced magnetic fields [112], or galactic winds [237].

The concomitant production of gamma-rays, associated with the neutrinos from SBG, must not exceed the non-blazar component of the extragalactic gamma-ray background (EGB) measured by Fermi-LAT [108]. This requirement constrains the properties of SBG emission [112,227,238], implying that the neutrino (and thus CR) spectrum must be sufficiently hard to explain the diffuse IceCube neutrinos above 100 TeV. This requirement can be somewhat relaxed by going beyond the "standard candle" approximation in which all SBGs have an identical neutrino and gamma-ray spectrum; even if only a fraction of SBGs have a sufficiently hard spectrum, they can still be consistent with the neutrino observations [43]. Refs. [230–232] conclude that the through-going muon neutrino flux at IceCube can indeed be explained by SBGs. We note that these conclusions are all based on a picture of CRs escaping the SBG mostly via advection from the strong winds. As noted by Ref. [239], if the amount of magnetic turbulence at the scales of CR gyroradii is suppressed due to ion-neutral damping, CRs may stream out of the SBG much faster, and thus largely suppress gamma-ray and neutrino production. However, this picture seems to be disfavored by the observation of TeV gamma-rays from various SBGs [240]. Finally, the possibility of observing individual SBGs as point sources of neutrinos remains open, although it appears that this requires much larger exposure than those available with IceCube, possibly achievable by IceCube-Gen2 and KM3NeT [234].

4.5. Galaxy Clusters

Galaxy clusters are the largest systems of gravitationally bound matter that are known in the Universe. Galaxy clusters as reservoirs of cosmic rays have been proposed for a long time [241–245]; possible sites for cosmic-ray acceleration are shock waves from large-scale structure formation or injection from sources inside the cluster, such as AGN, while intracluster gas, with a typical density of 10^{-4}–10^{-3} cm^{-3} is a natural target for

pp interaction. Galaxy clusters can thus act as reservoirs of CRs, confining them up to 100 PeV via magnetic diffusion, and therefore, leading to significant neutrino production. If cosmic rays are accelerated in accretion shocks, then galaxy clusters are disfavored as dominant sources of the IceCube neutrino flux by multiplet constraints [77] (see also Figure 2). Furthermore, they are in tension with multimessenger radio and gamma-ray observations, due to the expected soft cosmic-ray spectrum [246,247]; see, e.g., the argument in Section 3.4. On the other hand, if CRs are injected from sources inside the cluster with a sufficiently hard spectrum, they may be able to violate both these constraints [247] and be the dominant sources of IceCube neutrinos above 100 TeV [248,249]; intriguingly, in this scenario UHECRs might also be explained by the most energetic CRs above 100 PeV being able to escape the galaxy cluster [248,250], while the non-blazar component of the EGB would also be naturally explained by the gamma-rays produced together with neutrinos in pp interactions [248].

4.6. Cosmogenic Neutrinos

Regardless of what are the sources of UHECRs, a guaranteed contribution to the UHE neutrino flux comes from their interaction with the cosmic radiation background, composed of the cosmic microwave background (CMB) and the extragalactic background light (EBL), in the intergalactic space. Photohadronic collisions lead to the production of so-called cosmogenic neutrinos in the EeV energy range [251–256], and at the same time they cause a suppression of the UHECR flux, the Greizen–Zatsepin–Kuzmin (GZK) cutoff [257–259]. Recently, the contribution of leptonic processes has been proposed to lead to neutrino production at high redshifts if the center-of-mass energy for CR-photon collision is large enough to produce muons [260–263].

While the existence of cosmogenic neutrinos is guaranteed, the magnitude of their flux is largely uncertain. This uncertainty is mostly connected with the strong sensitivity to the maximum UHECR energy, their chemical composition—heavier nuclei produce typically lower cosmogenic neutrino fluxes—and the redshift evolution of their sources. In fact, while UHECRs observed on Earth are produced mainly at low redshifts, due to the attenuation by photohadronic energy losses, cosmogenic neutrinos reach Earth even from high redshifts. The chemical composition of UHECRs is subject to large uncertainties, although recent measurements from the Auger observatory [264–267] and Telescope Array (TA) [268] suggest a light composition at 1 EeV becoming heavier at higher energies. On the other hand, the redshift evolution of UHECR sources at high redshift has little impact on the UHECR flux itself, due to the GZK cutoff, and thus remains largely uncertain. Due to these uncertainties, the cosmogenic neutrino flux might be even lower than the UHE neutrino flux expected from certain astrophysical source classes.

Up to now, cosmogenic neutrinos have not been detected, and only upper bounds are available [154,269]. These bounds can already exclude optimistic predictions with redshift evolution stronger than star-formation rate and pure proton composition for the UHECRs. Future UHE neutrino telescopes, with their significantly improved sensitivity, might be able to detect the cosmogenic flux or rule out even less optimistic models.

4.7. Galactic Neutrinos

The existence of a diffuse galactic emission of neutrinos and gamma rays is essentially guaranteed by the simultaneous presence of propagating cosmic rays and interstellar material, which can act as a target for pp collisions. Thus, a Galactic neutrino flux has been widely discussed in literature [270–274]. This component is clearly anisotropic, due to the concentration of interstellar material near the galactic center and in the galactic disk. The intensity of this component depends on the interplay between the spatial distribution of cosmic-ray sources, the propagation model of cosmic rays, and the density of the target material. On general grounds, this flux is expected to rapidly decrease with energy as $\Phi_\nu \propto E_\nu^{-s_\nu}$ with s_ν close to 3, similar to the observed CR flux. However, the precise angular and spectral features of the flux depend on the interplay between the spatial

distribution of cosmic-ray sources, the propagation model of cosmic rays, and the density of the target material. Various determinations of the diffuse Galactic flux can be found, e.g., in Refs. [275–281].

The existence of a Galactic neutrino emission has been recently confirmed by the IceCube Collaboration [282] at the 4.5 σ level of significance. The magnitude of the Galactic component is small, contributing to ∼6–13% of the astrophysical flux at 30 TeV, explaining the challenging nature of the measurement. The observed spectrum is marginally consistent with the theoretically expected ones. The angular resolution of the sample also does not allow at present to claim whether the observed Galactic flux is truly diffuse or it comes from a superposition of many independently contributing sources [275,277,283–289], although upcoming neutrino telescopes may distinguish between the two scenarios by detecting neutrino multiplets from individual sources, see, e.g., Ref. [289].

5. Neutrinos Probing Beyond the Standard Model Physics

The high energies and large distances from Earth characterizing the production of astrophysical neutrinos make them an ideal probe for novel effects beyond the Standard Model (BSM). Because of their high energies, they are sensitive to non-standard couplings to new physics at large energy scales. Because of their large distances, even tiny BSM effects in their propagation can accumulate to produce sizable consequences. Here, we divide our discussion of the subject according to whether the BSM physics impacts the production, the propagation, or the detection process of astrophysical neutrinos.

5.1. BSM Effects on Neutrino Production

If neutrinos have novel, BSM couplings, there may be new channels for their production in high-energy astrophysical environments. A widely considered possibility is a (possibly indirect) coupling of neutrinos to heavy dark matter (DM) particles, with masses above 10–100 TeV. While DM should be stable over timescales comparable with the lifetime of the Universe, a sufficiently weak coupling to the Standard Model (SM) particles would still allow it to decay over longer timescales. If a DM particle decays into SM particles, neutrinos are generally produced, either because they are directly coupled to DM, or because the products of DM decay are energetic enough to initiate a showering of W and Z bosons [290] resulting in neutrino production. Therefore, the slow decay of galactic and extragalactic DM leads to a diffuse neutrino flux that should be observable by IceCube. It is easy to estimate the typical lifetimes that DM should have to produce a signal comparable with the IceCube sensitivity. Focusing for a moment on the Galactic DM component using the Galactic DM density $\rho_{\rm DM} \simeq 0.4\,{\rm GeV/cm^3}$, we infer from the dimensional analysis a neutrino flux of the order of

$$E_\nu^2 \frac{d\Phi_\nu}{dE_\nu d\Omega} \simeq \frac{\rho_{\rm DM} r_{\rm GC}}{4\pi\tau_{\rm DM}}, \tag{5}$$

where $r_{\rm GC} \simeq 10$ kpc is the typical length scale of our Galaxy. For a mass $m_{\rm DM} \simeq 1$ PeV, we find that lifetimes of the order of $\tau_{\rm DM} \simeq 10^{28}$–$10^{29}$ s lead to fluxes $E_\nu^2 d\Phi_\nu/dE_\nu d\Omega \simeq 10^{-8}$ GeV cm^{-2} s^{-1} sr^{-1}. For such lifetimes, IceCube could observe the neutrino signal from DM decay, essentially opening a new frontier of indirect DM detection. A similar scenario would be realized in models of annihilating DM [291–293], although the cross sections necessary to reach a flux comparable to IceCube sensitivity at $m_{\rm DM} \simeq 100$ TeV are beyond the unitarity limit [291,294,295].

This order-of-magnitude estimate guarantees that DM neutrinos could be observed by IceCube, but disentangling this signal from a more conventional astrophysical neutrino flux is more challenging. Indeed, in the early days of the IceCube measurements, DM was proposed as a possible explanation for the observed neutrino flux [296–307]. As a larger number of events was accumulated by IceCube, this scenario could be tested, using the characteristic features of DM neutrino fluxes compared to the more conventional astrophysical ones. DM neutrino fluxes are expected to be characteristically enhanced towards the Galactic Center, where a greater amount of Galactic DM resides, and to have

energy spectra sharply peaked around $E_\nu \simeq m_{\rm DM}/2$, the maximum energy that a neutrino can carry in each decay. Therefore, energy and angular-dependent studies of the IceCube data, assuming both a DM and an astrophysical component—the latter is typically modeled as a power-law flux—reveal that DM neutrinos could consistently explain a portion of the IceCube neutrinos, but are not significantly favored to a purely astrophysical explanation, see, e.g., Refs. [307,308]. Nevertheless, these analyses allow to draw lower bounds on the DM lifetime for decay in SM particles [292,293,309] which can be quite competitive with bounds drawn from gamma-ray measurements (e.g., Refs. [309–312]), especially in the case of primary decay to neutrinos. Furthermore, the sensitivity of the future radio telescopes to the diffuse flux of UHE neutrinos will allow them to extend these bounds into the region of heavier masses, above tens of PeV [309,313–315].

Besides providing a new channel for neutrino production, BSM physics might also impact the properties of the cosmic rays responsible for neutrino production. As an example, if cosmic rays possess non-standard interactions with sub-GeV DM, they might become scattered inside their sources, causing characteristic spectral distortions compared to their power-law spectrum. This possibility has been pointed out for Galactic cosmic rays in Ref. [316], and later extended also to extragalactic sources such as starburst galaxies [317]. If the cosmic-ray spectrum is distorted in such a way, the produced neutrinos would inherit the distortion and their spectrum would be affected; this possibility has been investigated for neutrinos produced in AGN in Ref. [318].

5.2. BSM Effects on Neutrino Propagation

In the standard picture, neutrinos propagate to Earth without sizable interactions, subject only to flavor mixing. Non-standard neutrino interactions may significantly distort this picture, affecting the energy, time, and angular distribution, as well as the flavor composition, of astrophysical neutrinos. The strong sensitivity to BSM effects mainly comes from the long baselines involved in neutrino propagation and in the high energies involved.

The first set of examples of BSM extensions that can be probed by this principle are non-standard neutrino–neutrino interactions, typically dubbed secret interactions. Astrophysical neutrinos propagate through a thermal bath of relic neutrinos from the early Universe, the cosmic neutrino background (CνB). Secret interactions provide a channel for astrophysical neutrinos to scatter off neutrinos from CνB. At each such scattering, a neutrino from the CνB is dragged into the direction of the astrophysical neutrino, while the energy is shared among both. When many such events accumulate over cosmological distances, the energy spectrum of astrophysical neutrinos is distorted. The possibility of probing secret interactions with high-energy astrophysical neutrino propagation, originally pointed out in the context of SN 1987A neutrinos [319], has been widely studied in the recent literature [320–331].

The quantitative relevance of this process depends, of course, on the magnitude of the cross-section for secret interaction, which must be determined from an underlying particle physics model. A common assumption is that the interaction is mediated by a new particle with mass m_ϕ, which directly determines the energy scale at which the new interaction would be phenomenologically relevant. Assuming that neutrinos from the CνB are at rest with a mass m_ν, the scattering with an astrophysical neutrino with energy E_ν becomes resonantly enhanced at an energy scale $E_\nu^{\rm res} \simeq m_\phi^2/m_\nu$. Assuming a neutrino mass $m_\nu \sim 0.1$ eV, with all three mass eigenstates having a similar mass scale for the range of mediator masses, $m_\phi \simeq 1$–10 MeV leads to a resonance neutrino energy visible in the IceCube range. Secret interactions would cause a characteristic dip in the neutrino energy spectrum around $E_\nu^{\rm res}$, as in the left panel of Figure 4. Since the total energy injected by astrophysical sources remains constant—while the neutrino number is not, as new neutrinos are dragged from the CνB—the neutrinos depleted around $E_\nu^{\rm res}$ pile up at lower energies. The absence of such distinctive energy features in the observed spectrum at IceCube can be used to constrain the strength of secret interactions, although there is an unavoidable degeneracy between the resonance energy $E_\nu^{\rm res}$ and the unknown mass scale

of the CNB neutrinos m_ν. For higher mediator masses, the scenario will be critically tested by future radio telescopes sensitive to UHE neutrinos [332]. Furthermore, if neutrinos in different flavor state couple with different strengths, energy-dependent flavor distortions could also be induced by the interaction [323,328]. Finally, since scattering events involve a small change in the neutrino direction, secret interactions could also induce a characteristic delay in the scattered neutrinos. Thus, if a neutrino signal were observed from a transient source, the neutrino light curve might, in principle, be used to probe this feature [333,334].

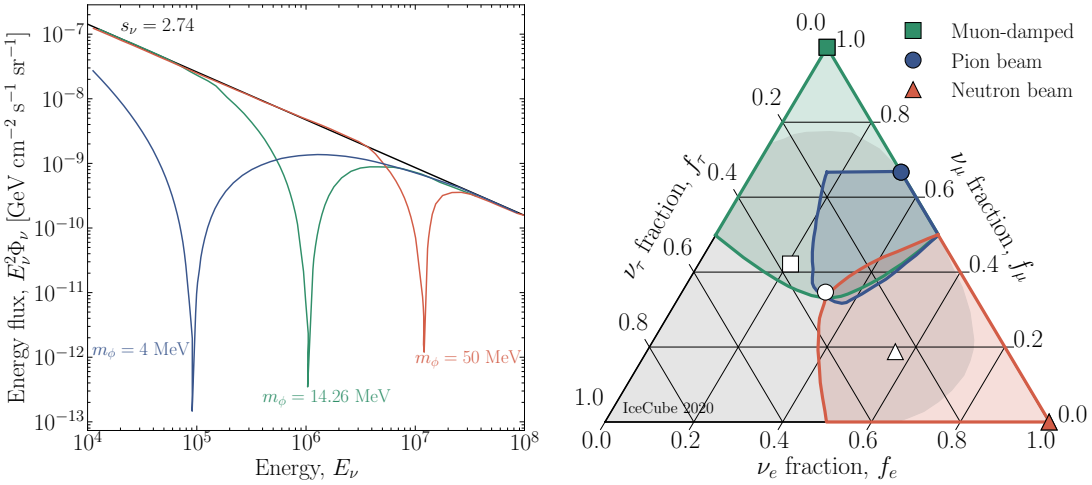

Figure 4. Examples of spectral and flavor distortions from BSM effects in extragalactic neutrino propagation. (**Left**) Spectral distortions induced by neutrino secret interactions with a mediator of mass m_ϕ; the characteristic dip is shown for various values of the m_ϕ. Figure reproduced from Ref. [331]. (**Right**) Allowed flavor composition from general BSM-induced flavor mixing with a generic unitary matrix $\tilde{U}$. Regions are shown for a source flavor composition corresponding to muon-damped (green), pion beam (blue), neutron beam (red); they are reproduced from Ref. [335]. The most recent IceCube constraints at 95% CL [88] are shown in gray.

A somewhat similar phenomenology can also be obtained in models with neutrinos oscillating into a fourth, sterile state, effectively disappearing. If the mass splitting with the new state is suitably tuned, the oscillation length may be comparable with the source distance, leading to a coherent energy dependence in the disappearance probability. This would show up in an energy-dependent modulation of the flux from point-like astrophysical neutrino sources, such as NGC 1068; this strategy has been proposed as a possible way to constrain scenarios with pseudo-Dirac neutrinos [323,336–345].

Flavor and spectral distortions might also be a way to probe non-standard neutrino decay. If the lifetime of a neutrino at rest is denoted by τ_ν, the expected number of neutrinos decaying over cosmological distances H_0^{-1}, where H_0 is Hubble's constant $m_\nu / \tau_\nu E_\nu H_0$, where the factor m_ν / E_ν accounts for the Lorentz dilatation. Thus, one can expect a sizable reduction jn the neutrino flux at energies below $E_\nu^{\rm dec} \simeq m_\nu / \tau_\nu H_0$. Depending on which mass eigenstate is unstable, the flux and flavor content at energies below $E_\nu^{\rm dec}$ is significantly affected, offering a new way to constrain the lifetime of decaying neutrinos [97,98,323,340,342,346–354].

Finally, non-standard neutrino mixing can also induce spectral and especially flavor distortions. Non-standard mixing can be induced by violation of fundamental symmetries, such as Lorentz invariance [355–358] or equivalence principle [359–363]. In the most general case, the neutrino Hamiltonian is extended to include novel couplings of the form $c_d \mathcal{V}_{\alpha\beta} E_\nu^{d-3} |\nu_\alpha\rangle\langle\nu_\beta|$, where α denotes flavor, c_d is an overall coupling with dimension GeV^{4-d}, d denotes the dimensionality of the operator, and $\mathcal{V}_{\alpha\beta}$ is a flavor structure matrix whose terms we assume to be of order unity. When the order of magnitude of the new couplings becomes larger than the typical mass-induced energy splittings $\delta m^2 / E_\nu$, where δm^2 is a typical scale of the squared mass splittings, the BSM terms become the dominant

ones in determining flavor mixing. Thus, below a characteristic energy $E_\nu^{\rm dist} \simeq (\delta m^2/c_d)^{\frac{1}{d-2}}$ the flavor composition is unaffected. Above $E_\nu^{\rm dist}$, the probabilities of flavor conversions are not determined by the mass matrix, but rather by the new matrix $\mathcal{V}$; this will be diagonalized by a new unitary matrix $\tilde{U}$, generally differing from the PMNS matrix U. Therefore, the flavor composition above $E_\nu^{\rm dist}$ is now only constrained by the unitarity of $\tilde{U}$; the general regions of parameter space that can be obtained for different production mechanisms are illustrated in Figure 4 (see Refs. [335,364,365]). The achievable flavor composition can extend even outside these unitarity bounds, e.g., in models with additional sterile neutrinos [366]. The intersection of the regions that can be obtained by varying $\tilde{U}$ with the confidence regions obtained by IceCube can help constrain the strength of these new interactions.

5.3. BSM Effects on Neutrino Detection

The detection of astrophysical neutrinos allows us to test the physics of neutrino interactions with nucleons in the Earth's crust and inside the detector. The neutrino–nucleon cross section at the large values of center-of-mass energy involved in each interaction cannot be tested in other terrestrial experiments, making the IceCube measurements a unique probe of this quantity. A larger neutrino–nucleon cross-section implies a larger number of neutrino interactions in the detector. However, the increase in the number of detected events degenerates with the unknown magnitude of the astrophysical flux—a larger number of events can be explained either by a larger cross-section or by a larger flux. On the other hand, the larger cross-section also implies an increased attenuation of the neutrinos passing through Earth. Therefore, the angular distribution of high-energy neutrinos around the horizon, where they are just able to pass through Earth, carries information about the neutrino–nucleon cross-section. This strategy has already been followed using the IceCube data [367–373], and its potential impact for the measurement of the neutrino–nucleon cross-section at UHE has been investigated in Refs. [374–377].

6. Summary

The main purpose of this work is to review briefly the recent advances in uncovering the origin of astrophysical high-energy neutrinos. After discussing the main processes by which such neutrinos can be produced within astrophysical sources, we have described how the properties of the neutrinos detected by IceCube—energy, position, flavor—can guide us in inferring the nature of their sources. To make the best use of these observations, however, they must be complemented by a multi-messenger view of the high-energy sky. Thus, we have reviewed how the connection with the high-energy gamma rays and ultra-high-energy cosmic rays provides significant constraints on what properties should the neutrino sources have. We have discussed, in particular, the main candidate astrophysical sources that could be responsible for the production of the bulk of or part of the diffuse high-energy neutrino flux. Throughout this discussion, we have emphasized the role that the future ultra-high-energy neutrino detectors may play in complementing the present view of the high-energy neutrino sky. Finally, we have shown how high-energy and ultra-high-energy neutrinos provide a learning opportunity to identify novel, non-standard interactions in the neutrino sector.

Funding: This research was funded by the Villum Fonden under Project No. 29388 and the European Union's Horizon 2020 Research and Innovation Program under the Marie Skłodowska-Curie Grant Agreement No. 847523 "INTERACTIONS".

Data Availability Statement: Data sharing is not applicable.

Acknowledgments: I am grateful to Antonio Ambrosone, Mauricio Bustamante, Antonio Capanema, Ersilia Guarini, Antonio Marinelli, Enrico Peretti, Tetyana Pitik for helpful comments and discussions.

Conflicts of Interest: The author declares no conflict of interest.

Abbreviations

The following abbreviations are used in this manuscript:

HE	High-energy
UHE	Ultra-high-energy
UHECR	Ultra-high-energy cosmic rays
CR	Cosmic rays
AGN	Active galactic nucleus
GRB	Gamma-ray burst
TDE	Tidal disruption event
SBG	Starburst galaxy
GC	Galaxy cluster
NP	Newborn pulsar
SNe	Supernovae
HNe	Hypernovae
FSRQ	Flat-spectrum radio quasar
LL	Low-luminosity
HL	High-luminosity
BSM	Beyond the Standard Model

References

1. Aartsen, M. et al. [IceCube Collaboration]. First observation of PeV-energy neutrinos with IceCube. *Phys. Rev. Lett.* **2013**, *111*, 021103. [CrossRef] [PubMed]
2. Aartsen, M. et al. [IceCube Collaboration]. Evidence for High-Energy Extraterrestrial Neutrinos at the IceCube Detector. *Science* **2013**, *342*, 1242856. [CrossRef] [PubMed]
3. Aartsen, M. et al. [IceCube Collaboration].Observation of High-Energy Astrophysical Neutrinos in Three Years of IceCube Data. *Phys. Rev. Lett.* **2014**, *113*, 101101. [CrossRef] [PubMed]
4. Aartsen, M. et al. [IceCube Collaboration]. Evidence for Astrophysical Muon Neutrinos from the Northern Sky with IceCube. *Phys. Rev. Lett.* **2015**, *115*, 081102. [CrossRef] [PubMed]
5. Aartsen, M. et al. [IceCube Collaboration]. Characteristics of the diffuse astrophysical electron and tau neutrino flux with six years of IceCube high energy cascade data. *Phys. Rev. Lett.* **2020**, *125*, 121104. [CrossRef]
6. Aartsen, M. et al. [IceCube Collaboration]. Neutrino emission from the direction of the blazar TXS 0506+056 prior to the IceCube-170922A alert. *Science* **2018**, *361*, 147. [CrossRef]
7. Aartsen, M. et al. [IceCube Collaboration]. Multimessenger observations of a flaring blazar coincident with high-energy neutrino IceCube-170922A. *Science* **2018**, *361*, eaat1378. [CrossRef]
8. Stein, R.; Velzen, S.V.; Kowalski, M.; Franckowiak, A.; Gezari, S.; Miller-Jones, J.C.; Frederick, S.; Sfaradi, I.; Bietenholz, M.F.; Horesh, A.; et al. A tidal disruption event coincident with a high-energy neutrino. *Nat. Astron.* **2021**, *5*, 510. [CrossRef]
9. Aartsen, M. et al. [IceCube Collaboration]. Time-Integrated Neutrino Source Searches with 10 Years of IceCube Data. *Phys. Rev. Lett.* **2020**, *124*, 051103. [CrossRef]
10. Abbasi, R. et al. [IceCube Collaboration]. Evidence for neutrino emission from the nearby active galaxy NGC 1068. *Science* **2022**, *378*, 538. [CrossRef]
11. Meszaros, P. Astrophysical Sources of High Energy Neutrinos in the IceCube Era. *Ann. Rev. Nucl. Part. Sci.* **2017**, *67*, 45. [CrossRef]
12. Vitagliano, E.; Tamborra, I.; Raffelt, G. Grand Unified Neutrino Spectrum at Earth: Sources and Spectral Components. *Rev. Mod. Phys.* **2020**, *92*, 45006. [CrossRef]
13. Kurahashi, N.; Murase, K.; Santander, M. High-Energy Extragalactic Neutrino Astrophysics. *Ann. Rev. Nucl. Part. Sci.* **2022**, *72*, 365. [CrossRef]
14. Fermi, E. On the Origin of the Cosmic Radiation. *Phys. Rev.* **1949**, *75*, 1169–1174. [CrossRef]
15. Drury, L.O. An introduction to the theory of diffusive shock acceleration of energetic particles in tenuous plasmas. *Rept. Prog. Phys.* **1983**, *46*, 973. [CrossRef]
16. Sjöstrand, T.; Ask, S.; Christiansen, J.R.; Corke, R.; Desai, N.; Ilten, P.; Mrenna, S.; Prestel, S.; Rasmussen, C.O.; Skands, P.Z. An introduction to PYTHIA 8.2. *Comput. Phys. Commun.* **2015**, *191*, 159. [CrossRef]
17. Ostapchenko, S. Monte Carlo treatment of hadronic interactions in enhanced Pomeron scheme: I. QGSJET-II model. *Phys. Rev. D* **2011**, *83*, 014018. [CrossRef]
18. Riehn, F.; Engel, R.; Fedynitch, A.; Gaisser, T.K.; Stanev, T. Hadronic interaction model Sibyll 2.3d and extensive air showers. *Phys. Rev. D* **2020**, *102*, 063002. [CrossRef]
19. Kelner, S.R.; Aharonian, F.A.; Bugayov, V.V. Energy spectra of gamma-rays, electrons and neutrinos produced at proton-proton interactions in the very high energy regime. *Phys. Rev. D* **2006**, *74*, 034018; Erratum in *Phys. Rev.* **2009**, *79*, 039901. [CrossRef]
20. Hummer, S.; Ruger, M.; Spanier, F.; Winter, W. Simplified models for photohadronic interactions in cosmic accelerators. *Astrophys. J.* **2010**, *721*, 630. [CrossRef]

21. Mucke, A.; Rachen, J.P.; Engel, R.; Protheroe, R.J.; Stanev, T. On photohadronic processes in astrophysical environments. *Publ. Astron. Soc. Austral.* **1999**, *16*, 160. [CrossRef]
22. Mücke, A.; Engel, R.; Rachen, J.P.; Protheroe, R.J.; Stanev, T. SOPHIA: Monte Carlo simulations of photohadronic processes in astrophysics. *Comput. Phys. Commun.* **2000**, *124*, 290. [CrossRef]
23. Winter, W. Neutrinos from Cosmic Accelerators Including Magnetic Field and Flavor Effects. *Adv. High Energy Phys.* **2012**, *2012*, 586413. [CrossRef]
24. Waxman, E.; Bahcall, J.N. High-energy neutrinos from cosmological gamma-ray burst fireballs. *Phys. Rev. Lett.* **1997**, *78*, 2292. [CrossRef]
25. Murase, K. High energy neutrino early afterglows gamma-ray bursts revisited. *Phys. Rev. D* **2007**, *76*, 123001. [CrossRef]
26. Hümmer, S.; Maltoni, M.; Winter, W.; Yaguna, C. Energy dependent neutrino flavor ratios from cosmic accelerators on the Hillas plot. *Astropart. Phys.* **2010**, *34*, 205. [CrossRef]
27. Dermer, C.D.; Murase, K.; Takami, H. Variable Gamma-ray Emission Induced by Ultra-High Energy Neutral Beams: Application to 4C +21.35. *Astrophys. J.* **2012**, *755*, 147. [CrossRef]
28. Fiorillo, D.F.G.; Vliet, A.V.; Morisi, S.; Winter, W. Unified thermal model for photohadronic neutrino production in astrophysical sources. *J. Cosmol. Astropart. Phys.* **2021**, *2021*, 028. [CrossRef]
29. Kelner, S.R.; Aharonian, F.A. Energy spectra of gamma-rays, electrons and neutrinos produced at interactions of relativistic protons with low energy radiation. *Phys. Rev. D* **2008**, *78*, 034013; Erratum in *Phys. Rev. D* **2010**, *82*, 099901. [CrossRef]
30. Fiorillo, D.F.G.; Bustamante, M. Bump hunting in the diffuse flux of high-energy cosmic neutrinos. *Phys. Rev. D* **2023**, *107*, 083008. [CrossRef]
31. Kashti, T.; Waxman, E. Flavoring astrophysical neutrinos: Flavor ratios depend on energy. *Phys. Rev. Lett.* **2005**, *95*, 181101. [CrossRef]
32. Lipari, P.; Lusignoli, M.; Meloni, D. Flavor Composition and Energy Spectrum of Astrophysical Neutrinos. *Phys. Rev. D* **2007**, *75*, 123005. [CrossRef]
33. Baerwald, P.; Hümmer, S.; Winter, W. Magnetic Field and Flavor Effects on the Gamma-Ray Burst Neutrino Flux. *Phys. Rev. D* **2011**, *83*, 067303. [CrossRef]
34. Baerwald, P.; Hummer, S.; Winter, W. Systematics in the Interpretation of Aggregated Neutrino Flux Limits and Flavor Ratios from Gamma-Ray Bursts. *Astropart. Phys.* **2012**, *35*, 508. [CrossRef]
35. Roulet, E.; Vissani, F. On the energy of the protons producing the very high-energy astrophysical neutrinos. *arXiv* **2020**, arXiv:2011.12769.
36. Aartsen, M.G. et al. [IceCube Collaboration]. Observation and Characterization of a Cosmic Muon Neutrino Flux from the Northern Hemisphere using six years of IceCube data. *Astrophys. J.* **2016**, *833*, 3. [CrossRef]
37. Ahlers, M.; Halzen, F. Opening a New Window onto the Universe with IceCube. *Prog. Part. Nucl. Phys.* **2018**, *102*, 73. [CrossRef]
38. Abbasi, R.U. et al. [IceCube Collaboration]. The IceCube high-energy starting event sample: Description and flux characterization with 7.5 years of data. *Phys. Rev. D* **2021**, *104*, 022002. [CrossRef]
39. Stettner, J. et al. [IceCube Collaboration]. Measurement of the Diffuse Astrophysical Muon-Neutrino Spectrum with Ten Years of IceCube Data. *Proc. Sci.* **2020**, *358*, 1017. [CrossRef]
40. Aartsen, M.G. et al. [IceCube Collaboration]. Measurements using the inelasticity distribution of multi-TeV neutrino interactions in IceCube. *Phys. Rev. D* **2019**, *99*, 032004. [CrossRef]
41. Abbasi, R. et al. [IceCube Collaboration]. Measurement of the astrophysical diffuse neutrino flux in a combined fit of IceCube's high energy neutrino data. *Proc. Sci.* **2023**, *444*, 1064. [CrossRef]
42. Palladino, A.; Winter, W. A multi-component model for observed astrophysical neutrinos. *Astron. Astrophys.* **2018**, *615*, A168. [CrossRef]
43. Ambrosone, A.; Chianese, M.; Fiorillo, D.F.G.; Marinelli, A.; Miele, G.; Pisanti, O. Starburst galaxies strike back: A multi-messenger analysis with Fermi-LAT and IceCube data. *Mon. Not. R. Astron. Soc.* **2021**, *503*, 4032. [CrossRef]
44. Telalovic, B.; Bustamante, M. Flavor Anisotropy in the High-Energy Astrophysical Neutrino Sky. *arXiv* **2023**, arXiv:2310.15224.
45. Fang, K.; Miller, M.C. A New Method for Finding Point Sources in High-energy Neutrino Data. *Astrophys. J.* **2016**, *826*, 102. [CrossRef]
46. Feyereisen, M.R.; Tamborra, I.; Ando, S. One-point fluctuation analysis of the high-energy neutrino sky. *J. Cosmol. Astropart. Phys.* **2017**, *2017*, 057. [CrossRef]
47. Aartsen, M.G. et al. [IceCube Collaboration]. Search for astrophysical sources of neutrinos using cascade events in IceCube. *Astrophys. J.* **2017**, *846*, 136. [CrossRef]
48. Capel, F.; Mortlock, D.J.; Finley, C. Bayesian constraints on the astrophysical neutrino source population from IceCube data. *Phys. Rev. D* **2020**, *101*, 123017; Erratum in *Phys. Rev. D* **2022**, *105*, 129904. [CrossRef]
49. Aartsen, M.G. et al. [IceCube Collaboration]. An All-Sky Search for Three Flavors of Neutrinos from Gamma-Ray Bursts with the IceCube Neutrino Observatory. *Astrophys. J.* **2016**, *824*, 115. [CrossRef]
50. Padovani, P.; Resconi, E.; Giommi, P.; Arsioli, B.; Chang, Y.L. Extreme blazars as counterparts of IceCube astrophysical neutrinos. *Mon. Not. R. Astron. Soc.* **2016**, *457*, 3582. [CrossRef]
51. Moharana, R.; Razzaque, S. Angular correlation between IceCube high-energy starting events and starburst sources. *J. Cosmol. Astropart. Phys.* **2016**, *2016*, 021. [CrossRef]

52. Resconi, E.; Coenders, S.; Padovani, P.; Giommi, P.; Caccianiga, L. Connecting blazars with ultrahigh-energy cosmic rays and astrophysical neutrinos. *Mon. Not. R. Astron. Soc.* **2017**, *468*, 597. [CrossRef]
53. Aartsen, M.G. et al. [IceCube Collaboration]. The contribution of Fermi-2LAC blazars to the diffuse TeV-PeV neutrino flux. *Astrophys. J.* **2017**, *835*, 45. [CrossRef]
54. Turley, C.F.; Fox, D.B.; Keivani, A.; DeLaunay, J.J.; Cowen, D.F.; Mostafa, M.; Solares, H.A.A.; Murase, K. A Coincidence Search for Cosmic Neutrino and Gamma-Ray Emitting Sources Using IceCube and *Fermi* LAT Public Data. *Astrophys. J.* **2018**, *863*, 64. [CrossRef]
55. Lunardini, C.; Vance, G.S.; Emig, K.L.; Windhorst, R.A. Are starburst galaxies a common source of high energy neutrinos and cosmic rays? *J. Cosmol. Astropart. Phys.* **2019**, *2019*, 073. [CrossRef]
56. Aartsen, M.G. et al. [IceCube Collaboration]. A Search for Neutrino Point-source Populations in 7 yr of IceCube Data with Neutrino-count Statistics. *Astrophys. J.* **2020**, *893*, 102. [CrossRef]
57. Plavin, A.; Kovalev, Y.Y.; Kovalev, Y.A.; Troitsky, S. Observational Evidence for the Origin of High-energy Neutrinos in Parsec-scale Nuclei of Radio-bright Active Galaxies. *Astrophys. J.* **2020**, *894*, 101. [CrossRef]
58. Buson, S.; Tramacere, A.; Pfeiffer, L.; Oswald, L.; de Menezes, R.; Azzollini, A.; Ajello, M. Beginning a Journey Across the Universe: The Discovery of Extragalactic Neutrino Factories. *Astrophys. J. Lett.* **2022**, *933*, L43; Erratum in *Astrophys. J. Lett.* **2022**, *934*, L38. [CrossRef]
59. Plavin, A.V.; Kovalev, Y.Y.; Kovalev, Y.A.; Troitsky, S.V. Growing evidence for high-energy neutrinos originating in radio blazars. *Mon. Not. R. Astron. Soc.* **2023**, *523*, 1799. [CrossRef]
60. Abbasi, R. et al. [IceCube Collaboration]. Search for Correlations of High-energy Neutrinos Detected in IceCube with Radio-bright AGN and Gamma-Ray Emission from Blazars. *Astrophys. J.* **2023**, *954*, 75. [CrossRef]
61. Buson, S.; Tramacere, A.; Oswald, L.; Barbano, E.; de Clairfontaine, G.F.; Pfeiffer, L.; Azzollini, A.; Baghmanyan, V.; Ajello, M. Extragalactic neutrino factories. *arXiv* **2023**, arXiv:2305.11263.
62. Bellenghi, C.; Padovani, P.; Resconi, E.; Giommi, P. Correlating High-energy IceCube Neutrinos with 5BZCAT Blazars and RFC Sources. *Astrophys. J. Lett.* **2023**, *955*, L32. [CrossRef]
63. Moharana, R.; Razzaque, S. Angular correlation of cosmic neutrinos with ultrahigh-energy cosmic rays and implications for their sources. *J. Cosmol. Astropart. Phys.* **2015**, *2015*, 014. [CrossRef]
64. Aartsen, M.G. et al. [IceCube, Pierre Auger, Telescope Array Collaboration]. Search for correlations between the arrival directions of IceCube neutrino events and ultrahigh-energy cosmic rays detected by the Pierre Auger Observatory and the Telescope Array. *J. Cosmol. Astropart. Phys.* **2016**, *2016*, 037. [CrossRef]
65. Albert, A. et al. [IceCube, Pierre Auger, Telescope Array, Auger, ANTARES Collaboration]. Search for Spatial Correlations of Neutrinos with Ultra-high-energy Cosmic Rays. *Astrophys. J.* **2022**, *934*, 164. [CrossRef]
66. Aartsen, M.G. et al. [IceCube Collaboration]. Searches for small-scale anisotropies from neutrino point sources with three years of IceCube data. *Astropart. Phys.* **2015**, *66*, 39. [CrossRef]
67. Aartsen, M.G. et al. [IceCube Collaboration]. Multipole analysis of IceCube data to search for dark matter accumulated in the Galactic halo. *Eur. Phys. J. C* **2015**, *75*, 20. [CrossRef]
68. Leuermann, M.; Schimp, M.; Wiebusch, C.H. Astrophysical interpretation of small-scale neutrino angular correlation searches with IceCube. *Astropart. Phys.* **2016**, *83*, 21. [CrossRef]
69. Dekker, A.; Ando, S. Angular power spectrum analysis on current and future high-energy neutrino data. *J. Cosmol. Astropart. Phys.* **2019**, *2019*, 002. [CrossRef]
70. Aartsen, M.G. et al. [IceCube Collaboration]. Searches for Time Dependent Neutrino Sources with IceCube Data from 2008 to 2012. *Astrophys. J.* **2015**, *807*, 46. [CrossRef]
71. Abbasi, R. et al. [IceCube Collaboration]. A Search for Time-dependent Astrophysical Neutrino Emission with IceCube Data from 2012 to 2017. *Astrophys. J.* **2021**, *911*, 67. [CrossRef]
72. Reusch, S.; Stein, R.; Kowalski, M.; Van Velzen, S.; Franckowiak, A.; Lunardini, C.; Murase, K.; Winter, W.; Miller-Jones, J.C.; Kasliwal, M.M.; et al. Candidate Tidal Disruption Event AT2019fdr Coincident with a High-Energy Neutrino. *Phys. Rev. Lett.* **2022**, *128*, 221101. [CrossRef] [PubMed]
73. van Velzen, S.; Stein, R.; Gilfanov, M.; Kowalski, M.; Hayasaki, K.; Reusch, S.; Yao, Y.; Garrappa, S.; Franckowiak, A.; Gezari, S.; et al. Establishing accretion flares from massive black holes as a major source of high-energy neutrinos. *arXiv* **2023**, arXiv:2111.09391.
74. Lipari, P. Proton and Neutrino Extragalactic Astronomy. *Phys. Rev. D* **2008**, *78*, 083011. [CrossRef]
75. Silvestri, A.; Barwick, S.W. Constraints on Extragalactic Point Source Flux from Diffuse Neutrino Limits. *Phys. Rev. D* **2010**, *81*, 023001. [CrossRef]
76. Ahlers, M.; Halzen, F. Pinpointing Extragalactic Neutrino Sources in Light of Recent IceCube Observations. *Phys. Rev. D* **2014**, *90*, 043005. [CrossRef]
77. Murase, K.; Waxman, E. Constraining High-Energy Cosmic Neutrino Sources: Implications and Prospects. *Phys. Rev. D* **2016**, *94*, 103006. [CrossRef]
78. Fang, K.; Kotera, K.; Miller, M.C.; Murase, K.; Oikonomou, F. Identifying Ultrahigh-Energy Cosmic-Ray Accelerators with Future Ultrahigh-Energy Neutrino Detectors. *J. Cosmol. Astropart. Phys.* **2016**, *2016*, 017. [CrossRef]
79. Fiorillo, D.F.G.; Bustamante, M.; Valera, V.B. Near-future discovery of point sources of ultra-high-energy neutrinos. *J. Cosmol. Astropart. Phys.* **2023**, *2023*, 026. [CrossRef]

80. Bartos, I.; Veske, D.; Kowalski, M.; Marka, Z.; Marka, S. The IceCube Pie Chart: Relative Source Contributions to the Cosmic Neutrino Flux. *Astrophys. J.* **2021**, *921*, 45. [CrossRef]
81. Ackermann, M.; Ahlers, M.; Anchordoqui, L.; Bustamante, M.; Connolly, A.; Deaconu, C.; Grant, D.; Gorham, P.; Halzen, F.; Karle, A. Astrophysics Uniquely Enabled by Observations of High-Energy Cosmic Neutrinos. *Bull. Am. Astron. Soc.* **2019**, *51*, 185.
82. Aartsen, M.G. et al. [IceCube Collaboration]. A combined maximum-likelihood analysis of the high-energy astrophysical neutrino flux measured with IceCube. *Astrophys. J.* **2015**, *809*, 98. [CrossRef]
83. Mena, O.; Palomares-Ruiz, S.; Vincent, A.C. Flavor Composition of the High-Energy Neutrino Events in IceCube. *Phys. Rev. Lett.* **2014**, *113*, 091103. [CrossRef] [PubMed]
84. Palomares-Ruiz, S.; Vincent, A.C.; Mena, O. Spectral analysis of the high-energy IceCube neutrinos. *Phys. Rev. D* **2015**, *91*, 103008. [CrossRef]
85. Aartsen, M.G. et al. [IceCube Collaboration]. Flavor Ratio of Astrophysical Neutrinos above 35 TeV in IceCube. *Phys. Rev. Lett.* **2015**, *114*, 171102. [CrossRef] [PubMed]
86. Palladino, A.; Vissani, F. The natural parameterization of cosmic neutrino oscillations. *Eur. Phys. J. C* **2015**, *75*, 433. [CrossRef]
87. Vincent, A.C.; Palomares-Ruiz, S.; Mena, O. Analysis of the 4-year IceCube high-energy starting events. *Phys. Rev. D* **2016**, *94*, 023009. [CrossRef]
88. Abbasi, R. et al. [IceCube Collaboration]. Detection of astrophysical tau neutrino candidates in IceCube. *Eur. Phys. J. C* **2022**, *82*, 1031. [CrossRef]
89. Aartsen, M.G. et al. [IceCube Collaboration]. Detection of a particle shower at the Glashow resonance with IceCube. *Nature* **2021**, *591*, 220; Erratum in *Nature* **2021**, *592*, E11. [CrossRef]
90. Biehl, D.; Fedynitch, A.; Palladino, A.; Weiler, T.J.; Winter, W. Astrophysical Neutrino Production Diagnostics with the Glashow Resonance. *J. Cosmol. Astropart. Phys.* **2017**, *2017*, 033. [CrossRef]
91. Liu, Q.; Song, N.; Vincent, A.C. Probing neutrino production in high-energy astrophysical neutrino sources with the Glashow resonance. *Phys. Rev. D* **2023**, *108*, 043022. [CrossRef]
92. Pontecorvo, B. Inverse beta processes and nonconservation of lepton charge. *Zh. Eksp. Teor. Fiz.* **1957**, *34*, 247.
93. Maki, Z.; Nakagawa, M.; Sakata, S. Remarks on the unified model of elementary particles. *Prog. Theor. Phys.* **1962**, *28*, 870–880. [CrossRef]
94. Rachen, J.P.; Meszaros, P. Photohadronic neutrinos from transients in astrophysical sources. *Phys. Rev. D* **1998**, *58*, 123005. [CrossRef]
95. Athar, H.; Jezabek, M.; Yasuda, O. Effects of neutrino mixing on high-energy cosmic neutrino flux. *Phys. Rev. D* **2000**, *62*, 103007. [CrossRef]
96. Crocker, R.M.; Melia, F.; Volkas, R.R. Searching for long wavelength neutrino oscillations in the distorted neutrino spectrum of galactic supernova remnants. *Astrophys. J. Suppl.* **2002**, *141*, 147. [CrossRef]
97. Barenboim, G.; Quigg, C. Neutrino observatories can characterize cosmic sources and neutrino properties. *Phys. Rev. D* **2003**, *67*, 073024. [CrossRef]
98. Beacom, J.F.; Bell, N.F.; Hooper, D.; Pakvasa, S.; Weiler, T.J. Measuring flavor ratios of high-energy astrophysical neutrinos. *Phys. Rev. D* **2003**, *68*, 093005; Erratum in *Phys. Rev. D* **2005**, *72*, 019901. [CrossRef]
99. Mena, O.; Mocioiu, I.; Razzaque, S. Oscillation effects on high-energy neutrino fluxes from astrophysical hidden sources. *Phys. Rev. D* **2007**, *75*, 063003. [CrossRef]
100. Esmaili, A.; Farzan, Y. An Analysis of Cosmic Neutrinos: Flavor Composition at Source and Neutrino Mixing Parameters. *Nucl. Phys. B* **2009**, *821*, 197. [CrossRef]
101. Choubey, S.; Rodejohann, W. Flavor Composition of UHE Neutrinos at Source and at Neutrino Telescopes. *Phys. Rev. D* **2009**, *80*, 113006. [CrossRef]
102. Winter, W. Photohadronic Origin of the TeV-PeV Neutrinos Observed in IceCube. *Phys. Rev. D* **2013**, *88*, 083007. [CrossRef]
103. Palladino, A.; Pagliaroli, G.; Villante, F.L.; Vissani, F. What is the Flavor of the Cosmic Neutrinos Seen by IceCube? *Phys. Rev. Lett.* **2015**, *114*, 171101. [CrossRef]
104. Bustamante, M.; Tamborra, I. Using high-energy neutrinos as cosmic magnetometers. *Phys. Rev. D* **2020**, *102*, 123008. [CrossRef]
105. Bustamante, M.; Ahlers, M. Inferring the flavor of high-energy astrophysical neutrinos at their sources. *Phys. Rev. Lett.* **2019**, *122*, 241101. [CrossRef]
106. Song, N.; Li, S.W.; Argüelles, C.A.; Bustamante, M.; Vincent, A.C. The Future of High-Energy Astrophysical Neutrino Flavor Measurements. *J. Cosmol. Astropart. Phys.* **2021**, *2021*, 054. [CrossRef]
107. Murase, K.; Fukugita, M. Energetics of High-Energy Cosmic Radiations. *Phys. Rev. D* **2019**, *99*, 063012. [CrossRef]
108. Ackermann, M. et al. [Fermi-LAT Collaboration]. The spectrum of isotropic diffuse gamma-ray emission between 100 MeV and 820 GeV. *Astrophys. J.* **2015**, *799*, 86. [CrossRef]
109. Fenu, F. [Pierre Auger Collaboration]. The cosmic ray energy spectrum measured using the Pierre Auger Observatory. *Proc. Sci* **2017**, *301*, 486. [CrossRef]
110. Waxman, E.; Bahcall, J.N. High-energy neutrinos from astrophysical sources: An Upper bound. *Phys. Rev. D* **1999**, *59*, 023002. [CrossRef]
111. Bahcall, J.N.; Waxman, E. High-energy astrophysical neutrinos: The Upper bound is robust. *Phys. Rev. D* **2001**, *64*, 023002. [CrossRef]

112. Murase, K.; Ahlers, M.; Lacki, B.C. Testing the Hadronuclear Origin of PeV Neutrinos Observed with IceCube. *Phys. Rev. D* **2013**, *88*, 121301. [CrossRef]
113. Murase, K.; Guetta, D.; Ahlers, M. Hidden Cosmic-Ray Accelerators as an Origin of TeV-PeV Cosmic Neutrinos. *Phys. Rev. Lett.* **2016**, *116*, 071101. [CrossRef] [PubMed]
114. Capanema, A.; Esmaili, A.; Murase, K. New constraints on the origin of medium-energy neutrinos observed by IceCube. *Phys. Rev. D* **2020**, *101*, 103012. [CrossRef]
115. Capanema, A.; Esmaili, A.; Serpico, P.D. Where do IceCube neutrinos come from? Hints from the diffuse gamma-ray flux. *J. Cosmol. Astropart. Phys.* **2021**, *2021*, 037. [CrossRef]
116. Mannheim, K.; Protheroe, R.J.; Rachen, J.P. On the cosmic ray bound for models of extragalactic neutrino production. *Phys. Rev. D* **2001**, *63*, 023003. [CrossRef]
117. Dermer, C.; Ramirez-Ruiz, E.; Le, T. Correlation of Photon and Neutrino Fluxes in Blazars and Gamma Ray Bursts. *Astrophys. J. Lett.* **2007**, *664*, L67. [CrossRef]
118. Murase, K.; Ioka, K.; Nagataki, S.; Nakamura, T. High-energy cosmic-ray nuclei from high- and low-luminosity gamma-ray bursts and implications for multi-messenger astronomy. *Phys. Rev. D* **2008**, *78*, 023005. [CrossRef]
119. Murase, K.; Ioka, K. TeV–PeV Neutrinos from Low-Power Gamma-Ray Burst Jets inside Stars. *Phys. Rev. Lett.* **2013**, *111*, 121102. [CrossRef] [PubMed]
120. Senno, N.; Murase, K.; Mészáros, P. Choked Jets and Low-Luminosity Gamma-Ray Bursts as Hidden Neutrino Sources. *Phys. Rev. D* **2016**, *93*, 083003. [CrossRef]
121. Kimura, S.S.; Murase, K.; Toma, K. Neutrino and Cosmic-Ray Emission and Cumulative Background from Radiatively Inefficient Accretion Flows in Low-Luminosity Active Galactic Nuclei. *Astrophys. J.* **2015**, *806*, 159. [CrossRef]
122. Murase, K.; Kimura, S.S.; Meszaros, P. Hidden Cores of Active Galactic Nuclei as the Origin of Medium-Energy Neutrinos: Critical Tests with the MeV Gamma-Ray Connection. *Phys. Rev. Lett.* **2020**, *125*, 011101. [CrossRef]
123. Inoue, Y.; Khangulyan, D.; Inoue, S.; Doi, A. On high-energy particles in accretion disk coronae of supermassive black holes: Implications for MeV gamma rays and high-energy neutrinos from AGN cores. *arXiv* **2019**, arXiv:1904.00554.
124. Kheirandish, A.; Murase, K.; Kimura, S.S. High-energy Neutrinos from Magnetized Coronae of Active Galactic Nuclei and Prospects for Identification of Seyfert Galaxies and Quasars in Neutrino Telescopes. *Astrophys. J.* **2021**, *922*, 45. [CrossRef]
125. Padovani, P.; Alexander, D.M.; Assef, R.J.; De Marco, B.; Giommi, P.; Hickox, R.C.; Richards, G.T.; Smolčić, V.; Hatziminaoglou, E.; Mainieri, V.; et al. Active galactic nuclei: What's in a name? *Astron. Astrophys. Rev.* **2017**, *25*, 2. [CrossRef]
126. Murase, K.; Stecker, F.W. High-Energy Neutrinos from Active Galactic Nuclei. In *The Encyclopedia of Cosmology*; World Scientific: Singapore, 2023; Chapter 10.
127. Berezinsky, V.S. Extraterestrial neutrino sources and high energy neutrino astrophysics. In Proceedings of the International Conference Neutrino '77, Baksan, Russia, 18–24 June 1977.
128. Silberberg, R.; Shapiro, M.M. Neutrinos as a Probe for the Nature of and Processes in Active Galactic Nuclei. In Proceedings of the International Cosmic Ray Conference, Kyoto, Japan, 6–18 August 1979; Volume 10, p. 357.
129. Eichler, D. High-energy neutrino astronomy: A probe of galactic nuclei? *Astrophys. J.* **1979**, *232*, 106. . [CrossRef]
130. Acciari, V.A.; Ansoldi, S.; Antonelli, L.A.; Engels, A.A.; Baack, D.; Babić, A.; Banerjee, B.; de Almeida, U.B.; Barrio, J.A.; González, J.B.; et al. Constraints on Gamma-Ray and Neutrino Emission from NGC 1068 with the MAGIC Telescopes. *Astrophys. J.* **2019**, *883*, 135. [CrossRef]
131. Berezinsky, V.S.; Ginzburg, V.L. On High Energy Neutrino Radiation of Quasars and Active Galactic Nuclei. In Proceedings of the International Cosmic Ray Conference, Paris, France, 13–25 July 1981; Volume 1, p. 238.
132. Inoue, Y.; Khangulyan, D.; Doi, A. On the Origin of High-energy Neutrinos from NGC 1068: The Role of Nonthermal Coronal Activity. *Astrophys. J. Lett.* **2020**, *891*, L33. [CrossRef]
133. Mbarek, R.; Philippov, A.; Chernoglazov, A.; Levinson, A.; Mushotzky, R. The Interplay between accelerated Protons, X-rays and Neutrinos in the Corona of NGC 1068: Constraints from Kinetic Plasma Simulations. *arXiv* **2023**, arXiv:2310.15222.
134. Fiorillo, D.F.G.; Petropoulou, M.; Comisso, L.; Peretti, E.; Sironi, L. TeV Neutrinos and Hard X-Rays from Relativistic Reconnection in the Corona of NGC 1068. *Astrophys. J.* **2024**, *961*, L14. [CrossRef]
135. Inoue, S.; Cerruti, M.; Murase, K.; Liu, R.-Y. High-energy neutrinos and gamma rays from winds and tori in active galactic nuclei. *arXiv* **2022**, arXiv:2207.02097. https://doi.org/10.48550/arXiv.2207.02097.
136. Fang, K.; Rodriguez, E.L.; Halzen, F.; Gallagher, J.S. High-energy Neutrinos from the Inner Circumnuclear Region of NGC 1068. *Astrophys. J.* **2023**, *956*, 8. [CrossRef]
137. Murase, K. Hidden Hearts of Neutrino Active Galaxies. *Astrophys. J. Lett.* **2022**, *941*, L17. [CrossRef]
138. Peretti, E.; Lamastra, A.; Saturni, F.G.; Ahlers, M.; Blasi, P.; Morlino, G.; Cristofari, P. Diffusive shock acceleration at EeV and associated multimessenger flux from ultra-fast outflows driven by active galactic nuclei. *Mon. Not. R. Astron. Soc.* **2023**, *526*, 181. [CrossRef]
139. Peretti, E.; Peron, G.; Tombesi, F.; Lamastra, A.; Saturni, F.G.; Cerruti, M.; Ahlers, M. Gamma-ray emission from the Seyfert galaxy NGC 4151 and multimessenger implications for ultra-fast outflows. *arXiv* **2023**, arXiv:2303.03298.
140. Mannheim, K. Neutrino signatures of the origins of cosmic rays. *Nucl. Phys. B Proc. Suppl.* **2014**, *256–257*, 264. [CrossRef]
141. Aharonian, F.A. TeV gamma-rays from BL Lac objects due to synchrotron radiation of extremely high-energy protons. *New Astron.* **2000**, *5*, 377. [CrossRef]

142. Mucke, A.; Protheroe, R.J. A Proton synchrotron blazar model for flaring in Markarian 501. *Astropart. Phys.* **2001**, *15*, 121. [CrossRef]
143. Mannheim, K.; Biermann, P.L. Photomeson production in active galactic nuclei. *Astron. Astrophys.* **1989**, *221*, 211.
144. Mannheim, K. The Proton blazar. *Astron. Astrophys.* **1993**, *269*, 67.
145. Atoyan, A.M.; Dermer, C.D. High-energy neutrinos from photomeson processes in blazars. *Phys. Rev. Lett.* **2001**, *87*, 221102. [CrossRef]
146. Murase, K.; Inoue, Y.; Dermer, C.D. Diffuse Neutrino Intensity from the Inner Jets of Active Galactic Nuclei: Impacts of External Photon Fields and the Blazar Sequence. *Phys. Rev. D* **2014**, *90*, 023007. [CrossRef]
147. Padovani, P.; Petropoulou, M.; Giommi, P.; Resconi, E. A simplified view of blazars: The neutrino background. *Mon. Not. R. Astron. Soc.* **2015**, *452*, 1877. [CrossRef]
148. Petropoulou, M.; Dimitrakoudis, S.; Padovani, P.; Mastichiadis, A.; Resconi, E. Photohadronic origin of γ-ray BL Lac emission: Implications for IceCube neutrinos. *Mon. Not. R. Astron. Soc.* **2015**, *448*, 2412. [CrossRef]
149. Halzen, F.; Zas, E. Neutrino fluxes from active galaxies: A Model independent estimate. *Astrophys. J.* **1997**, *488*, 669. [CrossRef]
150. Muecke, A.; Protheroe, R.J.; Engel, R.; Rachen, J.P.; Stanev, T. BL Lac Objects in the synchrotron proton blazar model. *Astropart. Phys.* **2003**, *18*, 593. [CrossRef]
151. Atoyan, A.M.; Dermer, C.D. Neutral beams from blazar jets. *Astrophys. J.* **2003**, *586*, 79. [CrossRef]
152. Rodrigues, X.; Heinze, J.; Palladino, A.; van Vliet, A.; Winter, W. Active Galactic Nuclei Jets as the Origin of Ultrahigh-Energy Cosmic Rays and Perspectives for the Detection of Astrophysical Source Neutrinos at EeV Energies. *Phys. Rev. Lett.* **2021**, *126*, 191101. [CrossRef] [PubMed]
153. Righi, C.; Palladino, A.; Tavecchio, F.; Vissani, F. EeV astrophysical neutrinos from flat spectrum radio quasars. *Astron. Astrophys.* **2020**, *642*, A92. [CrossRef]
154. Aartsen, M.G. et al. [IceCube Collaboration]. Differential limit on the extremely-high-energy cosmic neutrino flux in the presence of astrophysical background from nine years of IceCube data. *Phys. Rev. D* **2018**, *98*, 062003. [CrossRef]
155. Aartsen, M.G. et al. [IceCube Collaboration]. All-sky Search for Time-integrated Neutrino Emission from Astrophysical Sources with 7 yr of IceCube Data. *Astrophys. J.* **2017**, *835*, 151. [CrossRef]
156. Smith, D.; Hooper, D.; Vieregg, A. Revisiting AGN as the source of IceCube's diffuse neutrino flux. *J. Cosmol. Astropart. Phys.* **2021**, *2021*, 031. [CrossRef]
157. Yuan, C.; Murase, K.; Mészáros, P. Complementarity of Stacking and Multiplet Constraints on the Blazar Contribution to the Cumulative High-Energy Neutrino Intensity. *Astrophys. J.* **2020**, *890*, 25. [CrossRef]
158. Palladino, A.; Rodrigues, X.; Gao, S.; Winter, W. Interpretation of the diffuse astrophysical neutrino flux in terms of the blazar sequence. *Astrophys. J.* **2019**, *871*, 41. [CrossRef]
159. Ansoldi, S. et al. [MAGIC Collaboration]. The blazar TXS 0506+056 associated with a high-energy neutrino: Insights into extragalactic jets and cosmic ray acceleration. *Astrophys. J. Lett.* **2018**, *863*, L10. [CrossRef]
160. Keivani, A.; Murase, K.; Petropoulou, M.; Fox, D.B.; Cenko, S.B.; Chaty, S.; Coleiro, A.; DeLaunay, J.J.; Dimitrakoudis, S.; Evans, P.A. ; et al. A Multimessenger Picture of the Flaring Blazar TXS 0506+056: Implications for High-Energy Neutrino Emission and Cosmic Ray Acceleration. *Astrophys. J.* **2018**, *864*, 84. [CrossRef]
161. Murase, K.; Oikonomou, F.; Petropoulou, M. Blazar Flares as an Origin of High-Energy Cosmic Neutrinos? *Astrophys. J.* **2018**, *865*, 124. [CrossRef]
162. Cerruti, M.; Zech, A.; Boisson, C.; Emery, G.; Inoue, S.; Lenain, J.P. Leptohadronic single-zone models for the electromagnetic and neutrino emission of TXS 0506+056. *Mon. Not. R. Astron. Soc.* **2019**, *483*, L12; Erratum in *Mon. Not. R. Astron. Soc.* **2021**, *502*, L21–L22. [CrossRef]
163. Gao, S.; Fedynitch, A.; Winter, W.; Pohl, M. Modelling the coincident observation of a high-energy neutrino and a bright blazar flare. *Nat. Astron.* **2019**, *3*, 88. [CrossRef]
164. Reimer, A.; Boettcher, M.; Buson, S. Cascading Constraints from Neutrino-emitting Blazars: The Case of TXS 0506+056. *Astrophys. J.* **2019**, *881*, 46; Erratum in *Astrophys. J.* **2020**, *899*, 168. [CrossRef]
165. Rodrigues, X.; Gao, S.; Fedynitch, A.; Palladino, A.; Winter, W. Leptohadronic Blazar Models Applied to the 2014–2015 Flare of TXS 0506+056. *Astrophys. J. Lett.* **2019**, *874*, L29. [CrossRef]
166. Oikonomou, F.; Murase, K.; Padovani, P.; Resconi, E.; Mészáros, P. High energy neutrino flux from individual blazar flares. *Mon. Not. R. Astron. Soc.* **2019**, *489*, 4347. [CrossRef]
167. Zhang, B. *The Physics of Gamma-Ray Bursts*; Cambridge University Press: Cambridge, UK, 2018.
168. Meszaros, P. Gamma-Ray Bursts. *Rept. Prog. Phys.* **2006**, *69*, 2259. [CrossRef]
169. Kumar, P.; Zhang, B. The physics of gamma-ray bursts & relativistic jets. *Phys. Rept.* **2014**, *561*, 1. [CrossRef]
170. Vietri, M. On the acceleration of ultrahigh-energy cosmic rays in gamma-ray bursts. *Astrophys. J.* **1995**, *453*, 883. [CrossRef]
171. Waxman, E. Cosmological gamma-ray bursts and the highest energy cosmic rays. *Phys. Rev. Lett.* **1995**, *75*, 386. [CrossRef]
172. Baerwald, P.; Bustamante, M.; Winter, W. UHECR escape mechanisms for protons and neutrons from GRBs, and the cosmic ray-neutrino connection. *Astrophys. J.* **2013**, *768*, 186. [CrossRef]
173. Globus, N.; Allard, D.; Mochkovitch, R.; Parizot, E. UHECR acceleration at GRB internal shocks. *Mon. Not. R. Astron. Soc.* **2015**, *451*, 751. [CrossRef]

174. Baerwald, P.; Bustamante, M.; Winter, W. Are gamma-ray bursts the sources of ultra-high energy cosmic rays? *Astropart. Phys.* **2015**, *62*, 66. [CrossRef]
175. Bustamante, M.; Baerwald, P.; Murase, K.; Winter, W. Neutrino and cosmic-ray emission from multiple internal shocks in gamma-ray bursts. *Nat. Commun.* **2015**, *6*, 6783. [CrossRef]
176. Biehl, D.; Boncioli, D.; Fedynitch, A.; Winter, W. Cosmic-Ray and Neutrino Emission from Gamma-Ray Bursts with a Nuclear Cascade. *Astron. Astrophys.* **2018**, *611*, A101. [CrossRef]
177. Guetta, D.; Hooper, D.; Alvarez-Muniz, J.; Halzen, F.; Reuveni, E. Neutrinos from individual gamma-ray bursts in the BATSE catalog. *Astropart. Phys.* **2004**, *20*, 429. [CrossRef]
178. Li, Z. Note on the Normalization of Predicted GRB Neutrino Flux. *Phys. Rev. D* **2012**, *85*, 027301. [CrossRef]
179. Hummer, S.; Baerwald, P.; Winter, W. Neutrino Emission from Gamma-Ray Burst Fireballs, Revised. *Phys. Rev. Lett.* **2012**, *108*, 231101. [CrossRef] [PubMed]
180. He, H.-N.; Liu, R.-Y.; Wang, X.-Y.; Nagataki, S.; Murase, K.; Dai, Z.-G. Icecube non-detection of GRBs: Constraints on the fireball properties. *Astrophys. J.* **2012**, *752*, 29. [CrossRef]
181. Tamborra, I.; Ando, S. Inspecting the supernova–gamma-ray-burst connection with high-energy neutrinos. *Phys. Rev. D* **2016**, *93*, 053010. [CrossRef]
182. Tamborra, I.; Ando, S. Diffuse emission of high-energy neutrinos from gamma-ray burst fireballs. *J. Cosmol. Astropart. Phys.* **2015**, *2015*, 036. [CrossRef]
183. Bustamante, M.; Murase, K.; Winter, W.; Heinze, J. Multi-messenger light curves from gamma-ray bursts in the internal shock model. *Astrophys. J.* **2017**, *837*, 33. [CrossRef]
184. Liu, R.-Y.; Wang, X.-Y. Diffuse PeV neutrinos from gamma-ray bursts. *Astrophys. J.* **2013**, *766*, 73. [CrossRef]
185. Pitik, T.; Tamborra, I.; Petropoulou, M. Neutrino signal dependence on gamma-ray burst emission mechanism. *J. Cosmol. Astropart. Phys.* **2021**, *2021*, 034. [CrossRef]
186. Kimura, S.S. Neutrinos from Gamma-Ray Bursts. In *The Encyclopedia of Cosmology*; World Scientific: Singapore, 2023; Chapter 9.
187. Gao, S.; Asano, K.; Meszaros, P. High Energy Neutrinos from Dissipative Photospheric Models of Gamma Ray Bursts. *J. Cosmol. Astropart. Phys.* **2012**, *2012* , 058. [CrossRef]
188. Guarini, E.; Tamborra, I.; Gottlieb, O. State-of-the-art collapsar jet simulations imply undetectable subphotospheric neutrinos. *Phys. Rev. D* **2023**, *107*, 023001. [CrossRef]
189. Bahcall, J.N.; Meszaros, P. 5-GeV to 10-GeV neutrinos from gamma-ray burst fireballs. *Phys. Rev. Lett.* **2000**, *85*, 1362. [CrossRef] [PubMed]
190. Meszaros, P.; Rees, M.J. Multi GeV neutrinos from internal dissipation in GRB fireballs. *Astrophys. J. Lett.* **2000**, *541*, L5. [CrossRef]
191. Murase, K.; Kashiyama, K.; Mészáros, P. Subphotospheric Neutrinos from Gamma-Ray Bursts: The Role of Neutrons. *Phys. Rev. Lett.* **2013**, *111*, 131102. [CrossRef]
192. Waxman, E.; Bahcall, J.N. Neutrino afterglow from gamma-ray bursts: $\sim 10^{18}$ eV. *Astrophys. J.* **2000**, *541*, 707. [CrossRef]
193. Dai, Z.G.; Lu, T. Prompt neutrino emission from gamma-ray bursts. *Astrophys. J.* **2001**, *551*, 249. [CrossRef]
194. Dermer, C.D. Neutrino, neutron, and cosmic ray production in the external shock model of gamma-ray bursts. *Astrophys. J.* **2002**, *574*, 65. [CrossRef]
195. Guarini, E.; Tamborra, I.; Bégué, D.; Pitik, T.; Greiner, J. Multi-messenger detection prospects of gamma-ray burst afterglows with optical jumps. *J. Cosmol. Astropart. Phys.* **2022**, *2022*, 034. [CrossRef]
196. Adrian-Martinez, S. et al. [ANTARES Collaboration]. Search for muon neutrinos from gamma-ray bursts with the ANTARES neutrino telescope using 2008 to 2011 data. *Astron. Astrophys.* **2013**, *559*, A9. [CrossRef]
197. Aartsen, M.G. et al. [IceCube Collaboration]. Search for Prompt Neutrino Emission from Gamma-Ray Bursts with IceCube. *Astrophys. J. Lett.* **2015**, *805*, L5. [CrossRef]
198. Aartsen, M.G. et al. [IceCube Collaboration]. Extending the search for muon neutrinos coincident with gamma-ray bursts in IceCube data. *Astrophys. J.* **2017**, *843*, 112. [CrossRef]
199. Albert, A.; André, M.; Anghinolfi, M.; Anton, G.; Ardid, M.; Aubert, J.J.; Avgitas, T.; Baret, B.; Barrios-Martí, J.; Basa, S.; et al. Search for high-energy neutrinos from bright GRBs with ANTARES. *Mon. Not. R. Astron. Soc.* **2017**, *469*, 906. [CrossRef]
200. Albert, A. et al. [ANTARES Collaboration]. Constraining the contribution of Gamma-Ray Bursts to the high-energy diffuse neutrino flux with 10 yr of ANTARES data. *Mon. Not. R. Astron. Soc.* **2020**, *500*, 5614. [CrossRef]
201. IceCube Collaboration. GRB 221009A: Upper limits from a neutrino search with IceCube. In *GRB Coordinates Network*; No. 32665; NASA: Washington, DC, USA, 2022.
202. Liu, R.-Y.; Zhang, H.-M.; Wang, X.-Y. Constraints on Gamma-Ray Burst Models from GRB 221009A: GeV Gamma Rays versus High-energy Neutrinos. *Astrophys. J. Lett.* **2023**, *943*, L2. [CrossRef]
203. Murase, K.; Mukhopadhyay, M.; Kheirandish, A.; Kimura, S.S.; Fang, K. Neutrinos from the Brightest Gamma-Ray Burst? *Astrophys. J. Lett.* **2022**, *941*, L10. [CrossRef]
204. Ai, S.; Gao, H. Model Constraints Based on the IceCube Neutrino Nondetection of GRB 221009A. *Astrophys. J.* **2023**, *944*, 115. [CrossRef]
205. Murase, K.; Ioka, K.; Nagataki, S.; Nakamura, T. High Energy Neutrinos and Cosmic-Rays from Low-Luminosity Gamma-Ray Bursts? *Astrophys. J. Lett.* **2006**, *651*, L5. [CrossRef]

206. Gupta, N.; Zhang, B. Neutrino Spectra from Low and High Luminosity Populations of Gamma Ray Bursts. *Astropart. Phys.* **2007**, *27*, 386. [CrossRef]
207. Wang, X.-Y.; Razzaque, S.; Mészáros, P.; Dai, Z.-G. High-energy Cosmic Rays and Neutrinos from Semi-relativistic Hypernovae. *Phys. Rev. D* **2007**, *76*, 083009. [CrossRef]
208. Giannios, D.; Metzger, B.D.; Cenko, S.B.; Perley, D.A.; Butler, N.R.; Tanvir, N.R.; Levan, A.J.; O'Brien, P.T.; Strubbe, L.E.; et al. A relativistic jetted outburst from a massive black hole fed by a tidally disrupted star. *Science* **2011**, *333*, 203. [CrossRef]
209. Wang, X.-Y.; Liu, R.-Y. Tidal disruption jets of supermassive black holes as hidden sources of cosmic rays: Explaining the IceCube TeV-PeV neutrinos. *Phys. Rev. D* **2016**, *93*, 083005. [CrossRef]
210. Senno, N.; Murase, K.; Mészáros, P. High-energy Neutrino Flares from X-Ray Bright and Dark Tidal Disruption Events. *Astrophys. J.* **2017**, *838*, 3. [CrossRef]
211. Dai, L.; Fang, K. Can tidal disruption events produce the IceCube neutrinos? *Mon. Not. R. Astron. Soc.* **2017**, *469*, 1354. [CrossRef]
212. Lunardini, C.; Winter, W. High Energy Neutrinos from the Tidal Disruption of Stars. *Phys. Rev. D* **2017**, *95*, 123001. [CrossRef]
213. Murase, K.; Kimura, S.S.; Zhang, B.T.; Oikonomou, F.; Petropoulou, M. High-Energy Neutrino and Gamma-Ray Emission from Tidal Disruption Events. *Astrophys. J.* **2020**, *902*, 108. [CrossRef]
214. Hayasaki, K. Neutrinos from tidal disruption events. *arXiv* **2021**, arXiv:2102.11879.
215. Farrar, G.R.; Gruzinov, A. Giant AGN Flares and Cosmic Ray Bursts. *Astrophys. J.* **2009**, *693*, 329. [CrossRef]
216. Farrar, G.R.; Piran, T. Tidal disruption jets as the source of Ultra-High Energy Cosmic Rays. *arXiv* **2014**, arXiv:1411.0704.
217. Pitik, T.; Tamborra, I.; Angus, C.R.; Auchettl, K. Is the High-energy Neutrino Event IceCube-200530A Associated with a Hydrogen-rich Superluminous Supernova? *Astrophys. J.* **2022**, *929*, 163. [CrossRef]
218. Liu, R.-Y.; Xi, S.-Q.; Wang, X.-Y. Neutrino emission from an off-axis jet driven by the tidal disruption event AT2019dsg. *Phys. Rev. D* **2020**, *102*, 083028. [CrossRef]
219. Winter, W.; Lunardini, C. A concordance scenario for the observed neutrino from a tidal disruption event. *Nat. Astron.* **2021**, *5*, 472. [CrossRef]
220. Wu, H.-J.; Mou, G.; Wang, K.; Wang, W.; Li, Z. Could TDE outflows produce the PeV neutrino events? *Mon. Not. R. Astron. Soc.* **2022**, *514*, 4406. [CrossRef]
221. Winter, W.; Lunardini, C. Interpretation of the Observed Neutrino Emission from Three Tidal Disruption Events. *Astrophys. J.* **2023**, *948*, 42. [CrossRef]
222. Gao, Y.; Solomon, P.M. The Star formation rate and dense molecular gas in galaxies. *Astrophys. J.* **2004**, *606*, 271. [CrossRef]
223. Thomas, T.; Pfrommer, C.; Pakmor, R. Cosmic-ray-driven galactic winds: Transport modes of cosmic rays and Alfvén-wave dark regions. *Mon. Not. R. Astron. Soc.* **2023**, *521*, 3023. [CrossRef]
224. Ruszkowski, M.; Pfrommer, C. Cosmic ray feedback in galaxies and galaxy clusters: A pedagogical introduction and a topical review of the acceleration, transport, observables, and dynamical impact of cosmic rays. *Astron. Astrophys. Rev.* **2023**, *31*, 4. [CrossRef]
225. Loeb, A.; Waxman, E. The Cumulative background of high energy neutrinos from starburst galaxies. *J. Cosmol. Astropart. Phys.* **2006**, *2006*, 003. [CrossRef]
226. Thompson, T.A.; Quataert, E.; Waxman, E.; Loeb, A. Assessing The Starburst Contribution to the Gamma-Ray and Neutrino Backgrounds. *arXiv* **2006**, arXiv:astro-ph/0608699.
227. Tamborra, I.; Ando, S.; Murase, K. Star-forming galaxies as the origin of diffuse high-energy backgrounds: Gamma-ray and neutrino connections, and implications for starburst history. *J. Cosmol. Astropart. Phys.* **2014**, *2014*, 043. . [CrossRef]
228. Chang, X.-C.; Wang, X.-Y. The diffuse gamma-ray flux associated with sub-PeV/PeV neutrinos from starburst galaxies. *Astrophys. J.* **2014**, *793*, 131. [CrossRef]
229. Chakraborty, S.; Izaguirre, I. Star-forming galaxies as the origin of IceCube neutrinos: Reconciliation with Fermi-LAT gamma rays. *arXiv* **2016**, arXiv:1607.03361.
230. Palladino, A.; Fedynitch, A.; Rasmussen, R.W.; Taylor, A.M. IceCube Neutrinos from Hadronically Powered Gamma-Ray Galaxies. *J. Cosmol. Astropart. Phys.* **2019**, *2019*, 004. [CrossRef]
231. Peretti, E.; Blasi, P.; Aharonian, F.; Morlino, G. Cosmic ray transport and radiative processes in nuclei of starburst galaxies. *Mon. Not. R. Astron. Soc.* **2019**, *487*, 168. [CrossRef]
232. Peretti, E.; Blasi, P.; Aharonian, F.; Morlino, G.; Cristofari, P. Contribution of starburst nuclei to the diffuse gamma-ray and neutrino flux. *Mon. Not. R. Astron. Soc.* **2020**, *493*, 5880. [CrossRef]
233. Ha, J.-H.; Ryu, D.; Kang, H. Modeling of Cosmic-Ray Production and Transport and Estimation of Gamma-Ray and Neutrino Emissions in Starburst Galaxies. *arXiv* **2020**, arXiv:2008.06650.
234. Ambrosone, A.; Chianese, M.; Fiorillo, D.F.G.; Marinelli, A.; Miele, G. Could Nearby Star-forming Galaxies Light Up the Pointlike Neutrino Sky? *Astrophys. J. Lett.* **2021**, *919*, L32. [CrossRef]
235. Merckx, Y.; Correa, P.; de Vries, K.D.; Kotera, K.; Privon, G.C.; van Eijndhoven, N. Investigating starburst-driven neutrino emission from galaxies in the Great Observatories All-Sky LIRG Survey. *Phys. Rev. D* **2023**, *108*, 023015. [CrossRef]
236. Voelk, H.J. The correlation between radio and far-infrared emission for disk galaxies: A calorimeter theory. *Astron. Astrophys.* **1989**, *218*, 67.
237. Peretti, E.; Morlino, G.; Blasi, P.; Cristofari, P. Particle acceleration and multimessenger emission from starburst-driven galactic winds. *Mon. Not. R. Astron. Soc.* **2022**, *511*, 1336. [CrossRef]

238. Bechtol, K.; Ahlers, M.; Mauro, M.D.; Ajello, M.; Vandenbroucke, J. Evidence against star-forming galaxies as the dominant source of IceCube neutrinos. *Astrophys. J.* **2017**, *836*, 47. [CrossRef]
239. Krumholz, M.R.; Crocker, R.M.; Xu, S.; Lazarian, A.; Rosevear, M.; Bedwell-Wilson, J. Cosmic ray transport in starburst galaxies. *Mon. Not. R. Astron. Soc.* **2020**, *493*, 2817. [CrossRef]
240. Ambrosone, A.; Chianese, M.; Fiorillo, D.F.G.; Marinelli, A.; Miele, G. Observable signatures of cosmic rays transport in Starburst Galaxies on gamma-ray and neutrino observations. *Mon. Not. R. Astron. Soc.* **2022**, *515*, 5389. [CrossRef]
241. Volk, H.J.; Aharonian, F.A.; Breitschwerdt, D. The nonthermal energy content and gamma-ray emission of starburst galaxies and clusters of galaxies. *Space Sci. Rev.* **1996**, *75*, 279. [CrossRef]
242. Berezinsky, V.S.; Blasi, P.; Ptuskin, V.S. Clusters of Galaxies as a Storage Room for Cosmic Rays. *Astrophys. J.* **1997**, *487*, 529. [CrossRef]
243. Loeb, A.; Waxman, E. Gamma-ray background from structure formation in the intergalactic medium. *Nature* **2000**, *405*, 156. [CrossRef] [PubMed]
244. Keshet, U.; Waxman, E.; Loeb, A.; Springel, V.; Hernquist, L. Gamma-rays from intergalactic shocks. *Astrophys. J.* **2003**, *585*, 128. [CrossRef]
245. Kushnir, D.; Waxman, E. Nonthermal emission from clusters of galaxies. *J. Cosmol. Astropart. Phys.* **2009**, *2009*, 002. [CrossRef]
246. Zandanel, F.; Tamborra, I.; Gabici, S.; Ando, S. High-energy gamma-ray and neutrino backgrounds from clusters of galaxies and radio constraints. *Astron. Astrophys.* **2015**, *578*, A32. [CrossRef]
247. Fang, K.; Olinto, A.V. High-energy neutrinos from sources in clusters of galaxies. *Astrophys. J.* **2016**, *828*, 37. [CrossRef]
248. Fang, K.; Murase, K. Linking High-Energy Cosmic Particles by Black Hole Jets Embedded in Large-Scale Structures. *Nat. Phys.* **2018**, *14*, 396. [CrossRef]
249. Hussain, S.; Batista, R.A.; Pino, E.M.d.D.; Dolag, K. High-energy neutrino production in clusters of galaxies. *Mon. Not. R. Astron. Soc.* **2021**, *507*, 1762. [CrossRef]
250. Murase, K.; Inoue, S.; Nagataki, S. Cosmic Rays Above the Second Knee from Clusters of Galaxies and Associated High-Energy Neutrino Emission. *Astrophys. J. Lett.* **2008**, *689*, L105. [CrossRef]
251. Berezinsky, V.S.; Zatsepin, G.T. Cosmic rays at ultrahigh-energies (neutrino?). *Phys. Lett. B* **1969**, *28*, 423. [CrossRef]
252. Heinze, J.; Boncioli, D.; Bustamante, M.; Winter, W. Cosmogenic Neutrinos Challenge the Cosmic Ray Proton Dip Model. *Astrophys. J.* **2016**, *825*, 122. [CrossRef]
253. Aloisio, R.; Boncioli, D.; di Matteo, A.; Grillo, A.F.; Petrera, S.; Salamida, F. Cosmogenic neutrinos and ultra-high energy cosmic ray models. *J. Cosmol. Astropart. Phys.* **2015**, *2015*, 006. [CrossRef]
254. Ahlers, M.; Halzen, F. Minimal Cosmogenic Neutrinos. *Phys. Rev. D* **2012**, *86*, 083010. . [CrossRef]
255. Kotera, K.; Allard, D.; Olinto, A.V. Cosmogenic Neutrinos: Parameter space and detectabilty from PeV to ZeV. *J. Cosmol. Astropart. Phys.* **2010**, *2010*, 013. [CrossRef]
256. Allard, D.; Ave, M.; Busca, N.; Malkan, M.; Olinto, A.; Parizot, E.; Stecker, F.; Yamamoto, T. Cosmogenic Neutrinos from the propagation of Ultrahigh Energy Nuclei. *J. Cosmol. Astropart. Phys.* **2006**, *2006*, 005. [CrossRef]
257. Greisen, K. End to the cosmic ray spectrum? *Phys. Rev. Lett.* **1966**, *16*, 748. [CrossRef]
258. Zatsepin, G.T.; Kuzmin, V.A. Upper limit of the spectrum of cosmic rays. *JETP Lett.* **1966**, *4*, 78.
259. Abbasi, R.U. et al. [HiRes Collaboration]. First observation of the Greisen-Zatsepin-Kuzmin suppression. *Phys. Rev. Lett.* **2008**, *100*, 101101. [CrossRef]
260. Athar, H.; Lin, G.-L.; Tseng, J.-J. Muon pair production by electron photon scatterings. *Phys. Rev. D* **2001**, *64*, 071302. [CrossRef]
261. Li, Z.; Waxman, E. EeV neutrinos associated with UHECR sources. In Proceedings of the 32nd International Cosmic Ray Conference, Merida, Mexico, 3–11 July 2007; Volume 8, p. 262. [CrossRef]
262. Wang, K.; Liu, R.-Y.; Li, Z.; Dai, Z.-G. Neutrino Production in Electromagnetic Cascades: An extra component of cosmogenic neutrino at ultrahigh energies. *Phys. Rev. D* **2017**, *95*, 063010. [CrossRef]
263. Esmaeili, A.; Capanema, A.; Esmaili, A.; Serpico, P.D. Ultrahigh energy neutrinos from high-redshift electromagnetic cascades. *Phys. Rev. D* **2022**, *106*, 123016. [CrossRef]
264. Aab, A. et al. [Pierre Auger Collaboration]. Depth of maximum of air-shower profiles at the Pierre Auger Observatory. II. Composition implications. *Phys. Rev. D* **2014**, *90*, 122006. [CrossRef]
265. Aab, A. et al. [Pierre Auger Collaboration]. Evidence for a mixed mass composition at the 'ankle' in the cosmic-ray spectrum. *Phys. Lett. B* **2016**, *762*, 288. [CrossRef]
266. Aab, A. et al. [Pierre Auger Collaboration]. Combined fit of spectrum and composition data as measured by the Pierre Auger Observatory. *J. Cosmol. Astropart. Phys.* **2017**, *2017*, 038; Erratum in *J. Cosmol. Astropart. Phys.* **2018**, *2018*, E02. [CrossRef]
267. Aab, A. et al. [Pierre Auger Collaboration]. Inferences on mass composition and tests of hadronic interactions from 0.3 to 100 EeV using the water-Cherenkov detectors of the Pierre Auger Observatory. *Phys. Rev. D* **2017**, *96*, 122003. [CrossRef]
268. Abbasi, R.U. et al. [Telescope Array Collaboration]. Mass composition of ultrahigh-energy cosmic rays with the Telescope Array Surface Detector data. *Phys. Rev. D* **2019**, *99*, 022002. [CrossRef]
269. Aab, A. et al. [Pierre Auger Collaboration]. Probing the origin of ultra-high-energy cosmic rays with neutrinos in the EeV energy range using the Pierre Auger Observatory. *J. Cosmol. Astropart. Phys.* **2019**, *2019*, 022. [CrossRef]
270. Stecker, F.W. Diffuse Fluxes of Cosmic High-Energy Neutrinos. *Astrophys. J.* **1979**, *228*, 919. [CrossRef]
271. Domokos, G.; Elliott, B.; Kovesi-Domokos, S. Cosmic neutrino production in the Milky Way. *J. Phys. G* **1993**, *19*, 899. [CrossRef]

272. Berezinsky, V.S.; Gaisser, T.K.; Halzen, F.; Stanev, T. Diffuse radiation from cosmic ray interactions in the galaxy. *Astropart. Phys.* **1993**, *1*, 281. [CrossRef]
273. Ingelman, G.; Thunman, M.; Particle production in the interstellar medium. *arXiv* **1996**, arXiv:hep-ph/9604286.
274. Evoli, C.; Grasso, D.; Maccione, L. Diffuse Neutrino and Gamma-ray Emissions of the Galaxy above the TeV. *J. Cosmol. Astropart. Phys.* **2007**, *2007*, 003. [CrossRef]
275. Ahlers, M.; Murase, K. Probing the Galactic Origin of the IceCube Excess with Gamma-Rays. *Phys. Rev. D* **2014**, *90*, 023010. [CrossRef]
276. Gaggero, D.; Urbano, A.; Valli, M.; Ullio, P. Gamma-ray sky points to radial gradients in cosmic-ray transport. *Phys. Rev. D* **2015**, *91*, 083012. [CrossRef]
277. Ahlers, M.; Bai, Y.; Barger, V.; Lu, R. Galactic neutrinos in the TeV to PeV range. *Phys. Rev. D* **2016**, *93*, 013009. [CrossRef]
278. Gaggero, D.; Grasso, D.; Marinelli, A.; Urbano, A.; Valli, M. The gamma-ray and neutrino sky: A consistent picture of Fermi-LAT, Milagro, and IceCube results. *Astrophys. J. Lett.* **2015**, *815*, L25. [CrossRef]
279. Gaggero, D.; Grasso, D.; Marinelli, A.; Taoso, M.; Urbano, A. Diffuse cosmic rays shining in the Galactic center: A novel interpretation of H.E.S.S. and Fermi-LAT γ-ray data. *Phys. Rev. Lett.* **2017**, *119*, 031101. [CrossRef] [PubMed]
280. Albert, A. et al. [ANTARES Collaboration]. New constraints on all flavor Galactic diffuse neutrino emission with the ANTARES telescope. *Phys. Rev. D* **2017**, *96*, 062001. [CrossRef]
281. Aartsen, M.G. et al. [IceCube Collaboration]. Constraints on Galactic Neutrino Emission with Seven Years of IceCube Data. *Astrophys. J.* **2017**, *849*, 67. [CrossRef]
282. Abbasi, R. et al. [IceCube Collaboration]. Observation of high-energy neutrinos from the Galactic plane. *Science* **2023**, *380*, adc9818. [CrossRef]
283. Mandelartz, M.; Tjus, J.B. Prediction of the diffuse neutrino flux from cosmic ray interactions near supernova remnants. *Astropart. Phys.* **2015**, *65*, 80. [CrossRef]
284. Anchordoqui, L.A.; Goldberg, H.; Paul, T.C.; da Silva, L.H.M.; Vlcek, B.J. Estimating the contribution of Galactic sources to the diffuse neutrino flux. *Phys. Rev. D* **2014**, *90*, 123010. [CrossRef]
285. Fang, K.; Murase, K. Multi-messenger Implications of Sub-PeV Diffuse Galactic Gamma-Ray Emission. *arXiv* **2021**, arXiv:2104.09491.
286. Sudoh, T.; Beacom, J.F. Where are Milky Way's hadronic PeVatrons? *Phys. Rev. D* **2023**, *107*, 043002. [CrossRef]
287. Sudoh, T.; Beacom, J.F. Identifying Extended PeVatron Sources via Neutrino Shower Detection. *arXiv* **2023**, arXiv:2305.07043.
288. Schwefer, G.; Mertsch, P.; Wiebusch, C. Diffuse Emission of Galactic High-energy Neutrinos from a Global Fit of Cosmic Rays. *Astrophys. J.* **2023**, *949*, 16. [CrossRef]
289. Ambrosone, A.; Groth, K.M.; Peretti, E.; Ahlers, M. Galactic Diffuse Neutrino Emission from Sources beyond the Discovery Horizon. *arXiv* **2023**, arXiv:2306.17285.
290. Ciafaloni, P.; Comelli, D.; Riotto, A.; Sala, F.; Strumia, A.; Urbano, A. Weak Corrections are Relevant for Dark Matter Indirect Detection. *J. Cosmol. Astropart. Phys.* **2011**, *2011*, 019. [CrossRef]
291. Argüelles, C.A.; Diaz, A.; Kheirandish, A.; Olivares-Del-Campo, A.; Safa, I.; Vincent, A.C. Dark matter annihilation to neutrinos. *Rev. Mod. Phys.* **2021**, *93*, 035007. [CrossRef]
292. Abbasi, R. et al. [IceCube Collaboration]. Searches for Connections between Dark Matter and High-Energy Neutrinos with IceCube. *arXiv* **2022**, arXiv:2205.12950.
293. Abbasi, R. et al. [IceCube Collaboration]. Search for neutrino lines from dark matter annihilation and decay with IceCube. *arXiv* **2023**, arXiv:2303.13663.
294. Griest, K.; Kamionkowski, M. Unitarity Limits on the Mass and Radius of Dark Matter Particles. *Phys. Rev. Lett.* **1990**, *64*, 615. [CrossRef]
295. Smirnov, J.; Beacom, J.F. TeV-Scale Thermal WIMPs: Unitarity and its Consequences. *Phys. Rev. D* **2019**, *100*, 043029. [CrossRef]
296. Esmaili, A.; Serpico, P.D. Are IceCube neutrinos unveiling PeV-scale decaying dark matter? *J. Cosmol. Astropart. Phys.* **2013**, *2013*, 054. [CrossRef]
297. Feldstein, B.; Kusenko, A.; Matsumoto, S.; Yanagida, T.T. Neutrinos at IceCube from Heavy Decaying Dark Matter. *Phys. Rev. D* **2013**, *88*, 015004. [CrossRef]
298. Bai, Y.; Lu, R.; Salvadó, J. Geometric Compatibility of IceCube TeV-PeV Neutrino Excess and its Galactic Dark Matter Origin. *J. High Energy Phys.* **2016**, *2016*, 161. [CrossRef]
299. Ema, Y.; Jinno, R.; Moroi, T. Cosmic-Ray Neutrinos from the Decay of Long-Lived Particle and the Recent IceCube Result. *Phys. Lett. B* **2014**, *733*, 120. [CrossRef]
300. Esmaili, A.; Kang, S.K.; Serpico, P.D. IceCube events and decaying dark matter: Hints and constraints. *J. Cosmol. Astropart. Phys.* **2014**, *2014*, 054. [CrossRef]
301. Bhattacharya, A.; Reno, M.H.; Sarcevic, I. Reconciling neutrino flux from heavy dark matter decay and recent events at IceCube. *J. High Energy Phys.* **2014**, *2014*, 110. [CrossRef]
302. Murase, K.; Laha, R.; Ando, S.; Ahlers, M. Testing the Dark Matter Scenario for PeV Neutrinos Observed in IceCube. *Phys. Rev. Lett.* **2015**, *115*, 071301. [CrossRef] [PubMed]
303. Chianese, M.; Miele, G.; Morisi, S.; Vitagliano, E. Low energy IceCube data and a possible Dark Matter related excess. *Phys. Lett. B* **2016**, *757*, 251. [CrossRef]

304. Chianese, M.; Miele, G.; Morisi, S. Dark Matter interpretation of low energy IceCube MESE excess. *J. Cosmol. Astropart. Phys.* **2017**, *2017*, 007. [CrossRef]
305. Chianese, M.; Miele, G.; Morisi, S. Interpreting IceCube 6-year HESE data as an evidence for hundred TeV decaying Dark Matter. *Phys. Lett. B* **2017**, *773*, 591. [CrossRef]
306. Bhattacharya, A.; Esmaili, A.; Palomares-Ruiz, S.; Sarcevic, I. Update on decaying and annihilating heavy dark matter with the 6-year IceCube HESE data. *J. Cosmol. Astropart. Phys.* **2019**, *2019*, 051. [CrossRef]
307. Chianese, M.; Fiorillo, D.F.G.; Miele, G.; Morisi, S.; Pisanti, O. Decaying dark matter at IceCube and its signature on High Energy gamma experiments. *J. Cosmol. Astropart. Phys.* **2019**, *2019*, 046. [CrossRef]
308. Dekker, A.; Chianese, M.; Ando, S. Probing dark matter signals in neutrino telescopes through angular power spectrum. *J. Cosmol. Astropart. Phys.* **2020**, *2020*, 007. [CrossRef]
309. Argüelles, C.A.; Delgado, D.; Friedlander, A.; Kheirandish, A.; Safa, I.; Vincent, A.C.; White, H. Dark Matter decay to neutrinos. *arXiv* **2022**, arXiv:2210.01303.
310. Cohen, T.; Murase, K.; Rodd, N.L.; Safdi, B.R.; Soreq, Y. γ -ray Constraints on Decaying Dark Matter and Implications for IceCube. *Phys. Rev. Lett.* **2017**, *119*, 021102. [CrossRef] [PubMed]
311. Chianese, M.; Fiorillo, D.F.G.; Hajjar, R.; Miele, G.; Saviano, N. Constraints on heavy decaying dark matter with current gamma-ray measurements. *J. Cosmol. Astropart. Phys.* **2021**, *2021*, 035. [CrossRef]
312. Cao, Z. et al. [LHAASO Collaboration]. Constraints on Heavy Decaying Dark Matter from 570 Days of LHAASO Observations. *Phys. Rev. Lett.* **2022**, *129*, 261103. [CrossRef] [PubMed]
313. Guépin, C.; Aloisio, R.; Anchordoqui, L.A.; Cummings, A.; Krizmanic, J.F.; Olinto, A.V.; Reno, M.H.; Venters, T.M. Indirect dark matter searches at ultrahigh energy neutrino detectors. *Phys. Rev. D* **2021**, *104*, 083002. [CrossRef]
314. Chianese, M.; Fiorillo, D.F.G.; Hajjar, R.; Miele, G.; Morisi, S.; Saviano, N. Heavy decaying dark matter at future neutrino radio telescopes. *J. Cosmol. Astropart. Phys.* **2021**, *2021*, 074. [CrossRef]
315. Fiorillo, D.F.G.; Valera, V.B.; Bustamante, M.; Winter, W. Searches for dark matter decay with ultrahigh-energy neutrinos endure backgrounds. *Phys. Rev. D* **2023**, *108*, 103012. [CrossRef]
316. Cappiello, C.V.; Ng, K.C.Y.; Beacom, J.F. Reverse Direct Detection: Cosmic Ray Scattering with Light Dark Matter. *Phys. Rev. D* **2019**, *99*, 063004. [CrossRef]
317. Ambrosone, A.; Chianese, M.; Fiorillo, D.F.G.; Marinelli, A.; Miele, G. Starburst Galactic Nuclei as Light Dark Matter Laboratories. *Phys. Rev. Lett.* **2023**, *131*, 111003. [CrossRef]
318. Herrera, G.; Murase, K. Probing Light Dark Matter through Cosmic-Ray Cooling in Active Galactic Nuclei. *arXiv* **2023**, arXiv:2307.09460.
319. Kolb, E.W.; Turner, M.S. Supernova SN 1987a and the Secret Interactions of Neutrinos. *Phys. Rev. D* **1987**, *36*, 2895. [CrossRef]
320. Ioka, K.; Murase, K. IceCube PeV–EeV neutrinos and secret interactions of neutrinos. *PTEP* **2014**, *2014*, 061E01. [CrossRef]
321. Ng, K.C.Y.; Beacom, J.F. Cosmic neutrino cascades from secret neutrino interactions. *Phys. Rev. D* **2014**, *90*, 065035; Erratum In *Phys. Rev. D* **2014**, *90*, 089904. [CrossRef]
322. Ibe, M.; Kaneta, K. Cosmic neutrino background absorption line in the neutrino spectrum at IceCube. *Phys. Rev. D* **2014**, *90*, 053011. [CrossRef]
323. Shoemaker, I.M.; Murase, K. Probing BSM Neutrino Physics with Flavor and Spectral Distortions: Prospects for Future High-Energy Neutrino Telescopes. *Phys. Rev. D* **2016**, *93*, 085004. [CrossRef]
324. Kamada, A.; Yu, H.-B. Coherent Propagation of PeV Neutrinos and the Dip in the Neutrino Spectrum at IceCube. *Phys. Rev. D* **2015**, *92*, 113004. [CrossRef]
325. DiFranzo, A.; Hooper, D. Searching for MeV-Scale Gauge Bosons with IceCube. *Phys. Rev. D* **2015**, *92*, 095007. [CrossRef]
326. Kelly, K.J.; Machado, P.A.N. Multimessenger Astronomy and New Neutrino Physics. *J. Cosmol. Astropart. Phys.* **2018**, *2018*, 048. [CrossRef]
327. Barenboim, G.; Denton, P.B.; Oldengott, I.M. Constraints on inflation with an extended neutrino sector. *Phys. Rev. D* **2019**, *99*, 083515. [CrossRef]
328. Fiorillo, D.F.G.; Morisi, S.; Miele, G.; Saviano, N. Observable features in ultrahigh energy neutrinos due to active-sterile secret interactions. *Phys. Rev. D* **2020**, *102*, 083014. [CrossRef]
329. Creque-Sarbinowski, C.; Hyde, J.; Kamionkowski, M. Resonant neutrino self-interactions. *Phys. Rev. D* **2021**, *103*, 023527. [CrossRef]
330. Esteban, I.; Pandey, S.; Brdar, V.; Beacom, J.F. Probing secret interactions of astrophysical neutrinos in the high-statistics era. *Phys. Rev. D* **2021**, *104*, 123014. [CrossRef]
331. Bustamante, M.; Rosenstrøm, C.; Shalgar, S.; Tamborra, I. Bounds on secret neutrino interactions from high-energy astrophysical neutrinos. *Phys. Rev. D* **2020**, *101*, 123024. [CrossRef]
332. Fiorillo, D.F.G.; Miele, G.; Morisi, S.; Saviano, N. Cosmogenic neutrino fluxes under the effect of active-sterile secret interactions. *Phys. Rev. D* **2020**, *101*, 083024. [CrossRef]
333. Murase, K.; Shoemaker, I.M. Neutrino Echoes from Multimessenger Transient Sources. *Phys. Rev. Lett.* **2019**, *123*, 241102. [CrossRef]
334. Carpio, J.A.; Murase, K. Simulating neutrino echoes induced by secret neutrino interactions. *J. Cosmol. Astropart. Phys.* **2023**, *2023*, 042. [CrossRef]

335. Ahlers, M.; Bustamante, M.; Mu, S. Unitarity Bounds of Astrophysical Neutrinos. *Phys. Rev. D* **2018**, *98*, 123023. [CrossRef]
336. Beacom, J.F.; Bell, N.F.; Hooper, D.; Learned, J.G.; Pakvasa, S.; Weiler, T.J. PseudoDirac neutrinos: A Challenge for neutrino telescopes. *Phys. Rev. Lett.* **2004**, *92*, 011101. [CrossRef] [PubMed]
337. Keranen, P.; Maalampi, J.; Myyrylainen, M.; Riittinen, J. Effects of sterile neutrinos on the ultrahigh-energy cosmic neutrino flux. *Phys. Lett. B* **2003**, *574*, 162. [CrossRef]
338. Esmaili, A. Pseudo-Dirac Neutrino Scenario: Cosmic Neutrinos at Neutrino Telescopes. *Phys. Rev. D* **2010**, *81*, 013006. [CrossRef]
339. Esmaili, A.; Farzan, Y. Implications of the Pseudo-Dirac Scenario for Ultra High Energy Neutrinos from GRBs. *J. Cosmol. Astropart. Phys.* **2012**, *2012*, 014. [CrossRef]
340. Pakvasa, S.; Joshipura, A.; Mohanty, S. Explanation for the low flux of high energy astrophysical muon-neutrinos. *Phys. Rev. Lett.* **2013**, *110*, 171802. [CrossRef]
341. Joshipura, A.S.; Mohanty, S.; Pakvasa, S. Pseudo-Dirac neutrinos via a mirror world and depletion of ultrahigh energy neutrinos. *Phys. Rev. D* **2014**, *89*, 033003. [CrossRef]
342. Rasmussen, R.W.; Lechner, L.; Ackermann, M.; Kowalski, M.; Winter, W. Astrophysical neutrinos flavored with Beyond the Standard Model physics. *Phys. Rev. D* **2017**, *96*, 083018. [CrossRef]
343. Brdar, V.; Hansen, R.S.L. IceCube Flavor Ratios with Identified Astrophysical Sources: Towards Improving New Physics Testability. *J. Cosmol. Astropart. Phys.* **2019**, *2019*, 023. [CrossRef]
344. Rink, T.; Sen, M. Constraints on pseudo-Dirac neutrinos using high-energy neutrinos from NGC 1068. *arXiv* **2022**, arXiv:2211.16520.
345. Carloni, K.; Arguelles, C.A.; Martinez-Soler, I.; Babu, K.S.; Dev, P.S.B. Probing Pseudo-Dirac Neutrinos with Astrophysical Sources at IceCube. *arXiv* **2022**, arXiv:2212.00737.
346. Beacom, J.F.; Bell, N.F.; Hooper, D.; Pakvasa, S.; Weiler, T.J. Decay of High-Energy Astrophysical Neutrinos. *Phys. Rev. Lett.* **2003**, *90*, 181301. [CrossRef] [PubMed]
347. Meloni, D.; Ohlsson, T. Neutrino flux ratios at neutrino telescopes: The Role of uncertainties of neutrino mixing parameters and applications to neutrino decay. *Phys. Rev. D* **2007**, *75*, 125017. [CrossRef]
348. Maltoni, M.; Winter, W. Testing neutrino oscillations plus decay with neutrino telescopes. *J. High Energy Phys.* **2008**, *2008*, 064. [CrossRef]
349. Bustamante, M.; Gago, A.M.; Pena-Garay, C.P. Energy-Independent New Physics in the Flavour Ratios of High-Energy Astrophysical Neutrinos. *J. High Energy Phys.* **2010**, *2010*, 066. [CrossRef]
350. Baerwald, P.; Bustamante, M.; Winter, W. Neutrino Decays over Cosmological Distances and the Implications for Neutrino Telescopes. *J. Cosmol. Astropart. Phys.* **2012**, *2012*, 020. [CrossRef]
351. Dorame, L.; Miranda, O.G.; Valle, J.W.F. Invisible decays of ultra-high energy neutrinos. *Front. Phys.* **2013**, *1*, 25. [CrossRef]
352. Bustamante, M.; Beacom, J.F.; Winter, W. Theoretically palatable flavor combinations of astrophysical neutrinos. *Phys. Rev. Lett.* **2015**, *115*, 161302. [CrossRef]
353. Huang, Y.; Ma, B.-Q. Neutrino properties from ultra-high energy cosmic neutrinos. *Universe* **2015**, *3*, 15–21.
354. Bustamante, M.; Beacom, J.F.; Murase, K. Testing decay of astrophysical neutrinos with incomplete information. *Phys. Rev. D* **2017**, *95*, 063013. [CrossRef]
355. Argüelles, C.A.; Katori, T.; Salvadó, J. New Physics in Astrophysical Neutrino Flavor. *Phys. Rev. Lett.* **2015**, *115*, 161303. [CrossRef] [PubMed]
356. Aartsen, M.G. et al. [IceCube Collaboration]. Neutrino Interferometry for High-Precision Tests of Lorentz Symmetry with IceCube. *Nat. Phys.* **2018**, *14*, 961. [CrossRef]
357. Abbasi, R. et al. [IceCube Collaboration]. Search for quantum gravity using astrophysical neutrino flavour with IceCube. *Nat. Phys.* **2022**, *18*, 1287. [CrossRef]
358. Testagrossa, F.; Fiorillo, D.F.G.; Bustamante, M. Two-detector flavor sensitivity to ultra-high-energy cosmic neutrinos. *arXiv* **2023**, arXiv:2310.12215.
359. Gasperini, M. Experimental Constraints on a Minimal and Nonminimal Violation of the Equivalence Principle in the Oscillations of Massive Neutrinos. *Phys. Rev. D* **1989**, *39*, 3606. [CrossRef]
360. Sabbata, V.D.; Gasperini, M. Neutrino Oscillations in the Presence of Torsion. *Nuovo C. A* **1981**, *65*, 479. [CrossRef]
361. Glashow, S.L.; Halprin, A.; Krastev, P.I.; Leung, C.N.; Pantaleone, J.T. Comments on neutrino tests of special relativity. *Phys. Rev. D* **1997**, *56*, 2433. [CrossRef]
362. Minakata, H.; Smirnov, A.Y. High-energy cosmic neutrinos and the equivalence principle. *Phys. Rev. D* **1996**, *54*, 3698. [CrossRef] [PubMed]
363. Fiorillo, D.F.G.; Mangano, G.; Morisi, S.; Pisanti, O. IceCube constraints on violation of equivalence principle. *J. Cosmol. Astropart. Phys.* **2021**, *2021*, 079. [CrossRef]
364. Xu, X.-J.; He, H.-J.; Rodejohann, W. Constraining Astrophysical Neutrino Flavor Composition from Leptonic Unitarity. *J. Cosmol. Astropart. Phys.* **2014**, *2014*, 039. [CrossRef]
365. Fu, L.; Ho, C.M.; Weiler, T.J. Aspects of the Flavor Triangle for Cosmic Neutrino Propagation. *Phys. Rev. D* **2015**, *91*, 053001. [CrossRef]
366. Ahlers, M.; Bustamante, M.; Willesen, N.G.N. Flavors of astrophysical neutrinos with active-sterile mixing. *J. Cosmol. Astropart. Phys.* **2021**, *2021*, 029. [CrossRef]

367. Hooper, D. Measuring high-energy neutrino nucleon cross-sections with future neutrino telescopes. *Phys. Rev. D* **2002**, *65*, 097303. [CrossRef]
368. Hussain, S.; Marfatia, D.; McKay, D.W.; Seckel, D. Cross section dependence of event rates at neutrino telescopes. *Phys. Rev. Lett.* **2006**, *97*, 161101. [CrossRef]
369. Borriello, E.; Cuoco, A.; Mangano, G.; Miele, G.; Pastor, S.; Pisanti, O.; Serpico, P.D. Disentangling neutrino-nucleon cross section and high energy neutrino flux with a km^3 neutrino telescope. *Phys. Rev. D* **2008**, *77*, 045019. [CrossRef]
370. Hussain, S.; Marfatia, D.; McKay, D.W. Upward shower rates at neutrino telescopes directly determine the neutrino flux. *Phys. Rev. D* **2008**, *77*, 107304. [CrossRef]
371. Connolly, A.; Thorne, R.S.; Waters, D. Calculation of High Energy Neutrino-Nucleon Cross Sections and Uncertainties Using the MSTW Parton Distribution Functions and Implications for Future Experiments. *Phys. Rev. D* **2011**, *83*, 113009. [CrossRef]
372. Aartsen, M.G. et al. [IceCube Collaboration]. Measurement of the multi-TeV neutrino cross section with IceCube using Earth absorption. *Nature* **2017**, *551*, 596. [CrossRef]
373. Bustamante, M.; Connolly, A. Extracting the Energy-Dependent Neutrino-Nucleon Cross Section above 10 TeV Using IceCube Showers. *Phys. Rev. Lett.* **2019**, *122*, 041101. [CrossRef] [PubMed]
374. Marfatia, D.; McKay, D.W.; Weiler, T.J. New physics with ultra-high-energy neutrinos. *Phys. Lett. B* **2015**, *748*, 113. [CrossRef]
375. Valera, V.B.; Bustamante, M.; Glaser, C. The ultra-high-energy neutrino-nucleon cross section: Measurement forecasts for an era of cosmic EeV-neutrino discovery. *J. High Energy Phys.* **2022**, *2022*, 105. [CrossRef]
376. Esteban, I.; Prohira, S.; Beacom, J.F. Detector requirements for model-independent measurements of ultrahigh energy neutrino cross sections. *Phys. Rev. D* **2022**, *106*, 023021. [CrossRef]
377. Valera, V.B.; Bustamante, M.; Mena, O. Joint measurement of the ultra-high-energy neutrino spectrum and cross section. *arXiv* **2023**, arXiv:2308.07709.